Hdb Env Chem Vol. 2, Part N (2005): 1–x
DOI 10.1007/698_2_008

Published online:

Isotopic Tracers of the Marine Nitrogen Cycle: Present and Past

Mark A. Altabet

School for Marine Science and Technology, University of Massachusetts,
706 Rodney French Blvd, New Bedford, MA 02744-1221, USA
maltabet@umassd.edu

Abstract The oceanic nitrogen cycle consists of a web of microbially mediated transformations driven in part by the large range in possible nitrogen oxidation states. Many of these transformations have corresponding isotope fractionation effects, usually leaving the product depleted in ^{15}N ($\delta^{15}N$). Due to the complexity of the nitrogen cycle, observed patterns of isotopic ratio could be expected to defy explanation. However in reality, a few geographically separated processes dominate the larger spatial and temporal scales in the open ocean. These are (1) NO_3^- assimilation by phytoplankton, (2) N_2 fixation, and (3) denitrification. The latter two have particular importance as the principal source and sink, respectively, of combined nitrogen to the ocean. As such, they together control the oceanic inventory for combined nitrogen which in turn is a factor controlling marine plant production and organic matter flux from the surface to the ocean's interior. Taking into account the effective isotopic fractionation effects for N_2 fixation and denitrification, the modern average $\delta^{15}N$ for the ocean is a potentially important constraint

on the modern marine nitrogen budget. Past variation in these processes can be reconstructed on time scales from decades to millions of years from sediment cores with good preservation of organic matter. In particular, temporally well resolved $\delta^{15}N$ records show large variations in the three major water column denitrification regions in response to climate variations. Collectively, these variations in denitrification likely produced significant changes in the oceanic combined nitrogen inventory which appears to be confirmed by global-scale changes in $\delta^{15}N$ across the last deglaciation.

Keywords Nitrogen biogeochemistry · Denitrification · N_2 fixation · Stable isotope · Paleo-record

Abbreviations

‰	per mil
δ	"delta" convention for expressing natural variation in isotopic ratio
$\delta^{15}NO_3^-$	$\delta^{15}N$ of NO_3^-
ε	isotope fractionation factor
bp	before present
ACE	Antarctic climate event
DIN	dissolved inorganic nitrogen
D-O	Dansgaard–Oeschger event
ETNP	Eastern Tropical North Pacific
ETSP	Eastern Tropical South Pacific
f	fraction of remaining substrate
HNLC	high nutrient, low chlorophyll
kyr	kilo-year (10^3)
ka	kilo-annum (10^3)
MIS	marine isotope stage
Myr	mega-year (10^6)
N' or N*	NO_3^- concentration anomaly
OM	organic matter
OMZ	oxygen minimum zone
POM	particulate organic matter
SOM	sedimentary organic matter
Tg	Teragram (10^{12})

1 Overview

Nitrogen is a major component of biomass and the organic matter (OM) derived from it. Throughout much of the ocean, the availability of usable nitrogen is a dominant control of autotrophic production and OM fluxes. This control has ramifications for global biogeochemistry, in general, including influence on the oceanic C cycle and its forcing of atmospheric CO_2. Marine N biogeochemistry itself has a number of microbially mediated components which in combination regulate the combined N content of the ocean. In this Chapter, I will review these components and their N isotope fractionation ef-

fects. The use of the N isotope ratio as a natural tracer for marine N cycle processes then will be discussed, concluding with applications from the sediment record for past changes in relation to climate changes.

For convenience, the small but robust natural variations in $^{15}N : {}^{14}N$ ratio are typically reported using the "delta" notation employed for other stable isotope systems:

$$\delta^{15}N(‰) = (^{15}N : {}^{14}N_{sample} - {}^{15}N : {}^{14}N_{standard}) \; / {}^{15}N : {}^{14}N_{standard} \times 1000 \quad (1)$$

The accepted standard is atmospheric N_2 which by definition has a $\delta^{15}N$ of 0‰. In the oceans, combined N in its various forms can range between – 10 and + 15‰ with few examples of more extreme values. External analytical precision of environmental materials using modern techniques and instrumentation can be as good as ±0.1‰. The potential for N transformation processes to alter isotopic ratios is measured by the isotopic fractionation factor. Current literature typically refers to ε values which can be defined as:

$$\varepsilon(‰) = \delta^{15}N_{substrate} - \delta^{15}N_{product} \text{ or } \delta^{15}N_{product} = \delta^{15}N_{substrate} - \varepsilon \quad (2)$$

where there is no significant depletion of the substrate. Typically, ε values are between 0‰ (no isotope fractionation) and 40‰ for microbially mediated N transformation processes. That is, the product will usually have a lower $\delta^{15}N$ value than the substrate.

In a closed system with depletion of substrate and matching accumulation of product over time, the Rayleigh equations describe the change in isotope ratio as a function of the fraction of remaining substrate (f):

$$\delta^{15}N_{substrate}\,(f) = \delta^{15}N_{substrate}\,(f = 1) - \varepsilon \times \ln[f] \quad (3)$$

$$\delta^{15}N_{product}\,(f) = \delta^{15}N_{substrate}\,(f = 1) + \varepsilon \times f/[1 - f] \times \ln[f] \quad (4)$$

Modified Rayleigh equations are more appropriate to an open system akin to a chemostat with continual replenishment of substrate matched by removal of product:

$$\delta^{15}N_{substrate}\,(f) = \delta^{15}N_{substrate}\,(f = 1) + \varepsilon \times [1 - f] \quad (5)$$

$$\delta^{15}N_{product}\,(f) = \delta^{15}N_{substrate}\,(f = 1) - \varepsilon \times f \quad (6)$$

2 Dominant Marine N Processes and their Isotopic Effects

Nitrogen is found in nature at a variety of oxidation states giving rise to a large number of potential biogeochemical transformations and chemical forms. This large potential list is reduced by the environmental conditions

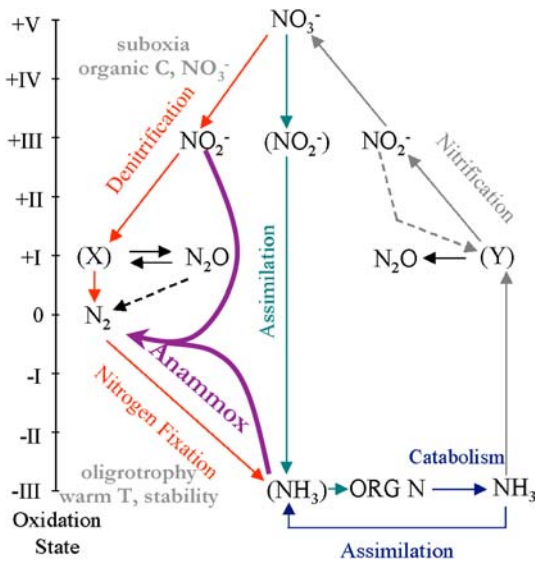

Fig. 1 Schematic representation of major nitrogen cycle paths based on an original Figure in [1]. The large range in nitrogen redox state is shown and is a factor in determining the circumstances under which any particular pathway is favorable. The recently discovered anammox pathway has been added

prevailing in today's ocean as well as the available biochemistries and the energy yield/requirement for particular transformations. While all significant transformations are biologically mediated, it is illustrative to present these with respect to redox state (Fig. 1 [1]). In the following discussion, the focus is on those processes with large-scale significance either with respect to oceanic N balance and/or creation of observed patterns in concentration.

2.1 N_2 fixation

In the form of dinitrogen gas (N_2), nitrogen is an abundant element on the Earth's surface. It makes up $\sim 80\%$ of the atmosphere by volume and is a similarly dominant component of dissolved gases in seawater. If this form of nitrogen could be directly used by all autotrophs, nitrogen availability would exert little or no control on marine (or any other) biogeochemistry and there would be little sense in writing this chapter. In reality, breaking the triple bond holding N_2 together is only mildly thermodynamically favorable ($\Delta G = -43\,\mathrm{kJ/mol\,N}$) with apparent large kinetic barriers and few groups of organisms possess the biochemical machinery, specifically the nitrogenase enzyme, to do so. Those capable of N_2 fixation are exclusively prokaryotes and N_2 fixing autotrophs fall within the cyanobacteria (blue-green algae). In

the ocean, the pelagic *Trichodesmium* species appear to be the dominant N_2 fixing organisms [2] followed by diatom endosymbionts (e.g. *Richelia*; see review by [3]).

The nitrogenase enzyme is both O_2 sensitive and has a high requirement for Fe [4]. The relative demand as compared to non-N_2 fixers, though, has been sharply revised downward to 4-fold [5]. Given the very low Fe concentrations found in the well-oxygenated open ocean of today and well-conserved structure of its active site across phylogenetic groupings, it has been suggested that nitrogenase evolved early in the Earth's history before oxygenation of the atmosphere several billion years ago [6]. O_2 sensitivity poses a problem for oxygenetic photoautotrophs with one solution being the formation of specialized non-photosynthetic, N_2 fixing cells referred to as heterocysts which have thickened cell walls to inhibit the inward diffusion of O_2. Despite its high O_2 environment in the near-surface open ocean, *Trichodesmium* lacks heterocysts and in fact couples photosynthetic energy production to N_2 fixation. How O_2 inhibition is overcome is not well understood.

The high requirement for Fe has further suggested an interaction between Fe and N biogeochemistry [6]. Since Fe is chiefly supplied by eolian dust input, proximity to these sources is thought to be a control on *Trichodesmium* population size and activity. Indeed, recent studies in the subtropical/tropical North Atlantic show *Trichodesmium* to be relatively Fe replete in this region which receives a large flux of Fe in the form of Saharan dust [7]. However, co-limitation with phosphorous has been reported [8]. Given the wide spatial variation in Fe delivery to the ocean's surface, it has been estimated that in 75% of the ocean's area, N_2 fixation is potentially limited by Fe [9].

N_2 fixers have a clear ecological advantage when the supply of combined N to photoautotrophs is very low. Hence, *Trichodesmium* blooms are typically found in oligotrophic parts of the ocean where high insolation, water column stability, and warm temperatures further favor this group of organisms. Assuming there is sufficient Fe, an apparent paradox is that low available combined N also implies a low flux of P. If *Trichodesmium* were constrained by the average (Redfield) ratio of N to P found in both phytoplankton and inorganic sources in deep water (16 : 1; [10]), little N_2 fixation could be accomplished before P limitation would set in. One possible solution would be faster recycling in near-surface waters of P as compared to combined N. However, recent field studies demonstrate that *Trichodesmium* N : P can be several fold higher than the Redfield ratio [7].

Since N_2 fixation contributes locally to regionally to the combined N inventory without any corresponding input of P, remineralization of relatively N rich OM results in subsurface NO_3^- : PO_4^{-3} ratios higher than the Redfield ratio. There are several formulations in the literature for quantifying the NO_3^- anomaly relative to PO_4^{-3} including the now well-known "N^*" parameter devised by Gruber and Sarmiento [11] and later modified by Deutsch

et al. [12]. I refer to my personal preference of N′ for its simplicity and lack of assumptions regarding the N : P ratio of decaying organic mater:

$$N' = NO_3^- + NO_2^- - 16 \times PO_4^{-3} \quad (7)$$

Regardless of the specific formulation, geochemical approaches using NO_3^- anomalies dramatically changed views regarding the magnitude of oceanic N_2 fixation such that it is now seen as clearly the predominant source of combined N to the ocean. Prior estimates were based on combinations of *Trichodesmium* abundance estimates and N_2 rate measurements made using incubation techniques (e.g. [2]). In hindsight, prior studies likely underestimated oceanic N_2 fixation due to undersampling of *Trichodesmium* activity that is highly variable in time and space. Geochemical approaches have the advantage of integrating over the time and space scales of the circulation and renewal of the subsurface waters in which the NO_3^- anomalies accumulate—years to decades and hundreds to thousands of km. As expected, the most positive N* or N′ values are found in subsurface waters (100 to 1000 m) underlying regions such as the Sargasso Sea where *Trichodesmium* blooms are known to regularly occur. However, estimation of pelagic marine N_2 fixation is far from settled in that recent work has suggested geochemical measures are closer to the prior biological ones due to smaller than assumed areal extent of the N* anomaly [13]. Large interannual variability in positive N* in the subsurface waters of the Sargasso Sea have also been observed [14] suggesting that temporal aliasing is also a concern with the geochemical approach.

Given the conservation of nitrogenase and presumably its catalytic mechanism and kinetics thereof, it is not surprising that fairly similar isotopic fractionation effects are observed for different phylogenetic groupings of N_2 fixers (e.g. [15–18]). Despite the energy required to break the triple bond in N_2, little discrimination against ^{15}N is observed, making the intracellular product NH_4^+ and subsequent organic N, similar in isotopic composition to the N_2 substrate. Regarding oceanic N_2 fixation, *Trichodesmium* isotopic composition can be measured directly to assess its impact on marine isotope biogeochemistry. Averages are between – 1 and – 2‰ [19, 20] consistent with small ε values of 2 to 3‰ given that the $\delta^{15}N$ of dissolved N_2 is about 0.7‰ higher than atmospheric N_2 (0‰ by definition) due to equilibrium isotopic fractionation between dissolved and gas phase N_2.

Average marine NO_3^- has a $\delta^{15}N$ value of $\sim$ 4.7‰ [21, 22]. The contributions from N_2 fixation that produce positive NO_3^- anomalies (N′) should also, by contributing ^{15}N depleted N, reduce NO_3^- $\delta^{15}N$ values ($\delta^{15}NO_3^-$) below 4.7‰. This is clearly seen in the subtropical N. Atlantic where the region of positive N′ between 100 and 1000 m corresponds to $\delta^{15}NO_3^-$ values as low as 1‰ (Fig. 2). These results reflect influence from N_2 fixation in overlying surface waters which produces OM with higher than average N : P and $\delta^{15}N$ lower than 4.7‰. When this OM sinks below 100 m and degrades to its inorganic constituents, positive N′ and lowered $\delta^{15}N$ NO_3^- values are pro-

duced. The region below 1000 m with slightly negative N′ has $\delta^{15}NO_3^-$ values indistinguishable from the oceanic average. This is sensible since almost all sinking organic particles are degraded above 1000 m.

If positive N′ quantitatively reflects the contribution from N_2 fixation then:

$$\delta^{15}NO_3^- = [N' \times -2 + (NO_3^- + NO_2^- - N') \times 4.7]/(NO_3^- + NO_2^-) \quad (8)$$

but rearranging for convenient plotting:

$$\delta^{15}NO_3^- = 4.7 - 6.7^*N'/(NO_3^- + NO_2^-) \quad (9)$$

Plotting the data in Fig. 2 as $\delta^{15}NO_3^-$ vs. N′/N (Fig. 3) shows points distributed about this expected trend confirming that N′ is a generally reliable indicator for contributions from N_2 fixation. Consequences for global N isotope balance and possible reconstruction of past N_2 fixation are discussed below. Very recent analytical improvements in measuring the $\delta^{15}NO_3^-$, particularly at concentrations below 2 μM, will likely reduce scatter in the data distribution [2]. These new techniques in which NO_3^- is converted to N_2O for mass spectrometric analysis preserves oxygen isotopic information which can be used to detect influence on $\delta^{15}N$ values by removal processes such as denitrification or phytoplankton NO_3^- assimilation [24].

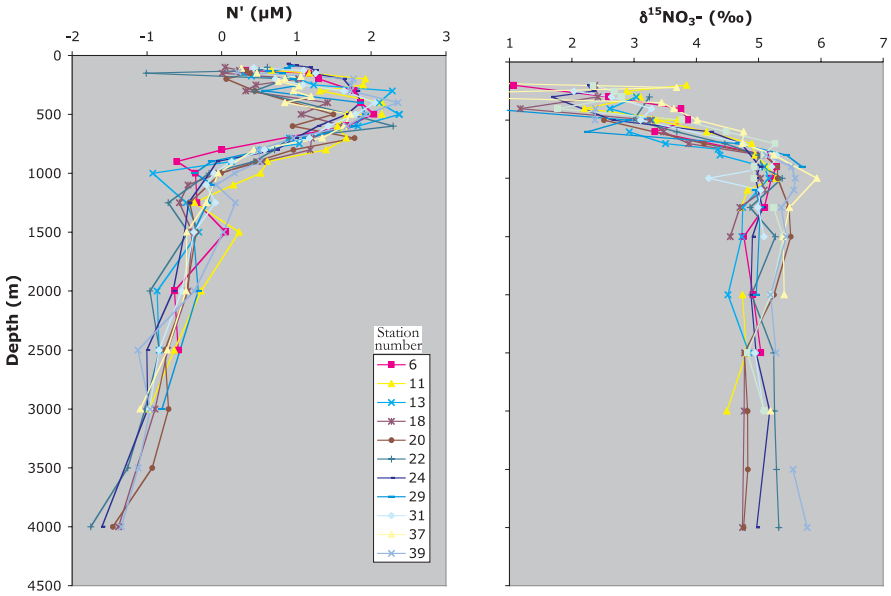

Fig. 2 Vertical profiles of N′ (see text) and $\delta^{15}NO_3^-$ from a series of stations in the Sargasso Sea (subtropical N. Pacific). The positive N′ values in the upper 1000 m are evidence for N_2 fixation in the overlaying surface waters. The relatively low $\delta^{15}NO_3^-$ values in this depth region are consistent with this perspective

2.2 Denitrification

If N_2 fixation is the entry point to the biosphere for combined N, then denitrification is the clear exit. In this case, its importance as a sink for combined N is incidental to its physiological significance. When O_2 falls to $< 5\,\mu M$, it becomes energy efficient for many heterotrophic bacteria to facultatively[CE a] use the denitrification pathway to respire OM with NO_3^- as an electron acceptor [25]:

$$(CH_2O)_{106}(NH_3)_{16}H_3PO_4 + 84.8\,HNO_3 = 106\,CO_2 + 42.4\,N_2 + 16\,NH_3 + 148.4\,H_2O + H_3PO_4 \quad (10)$$

The energy yield for this reaction ($\Delta G = -452$ kJ/mol C) is only slightly less than for aerobic respiration ($\Delta G = -476$ kJ/mol C). Only after NO_3^- is consumed are processes such as sulfate reduction with a much lower energy yield favored ($\Delta G = -82$ kJ/mol C). Thus the requirements for denitrification are (1) a supply of NO_3^-, (2) suboxic conditions, and (3) a supply of OM. Not surprisingly #'s 2 and 3 often co-occur. Also note that N_2O is an intracellular intermediate (Fig. 1) such that denitrification potentially can result in either net production or consumption. However, N_2O is usually well below saturation concentrations (assuming equilibrium with the atmosphere) within active denitrification zones [26].

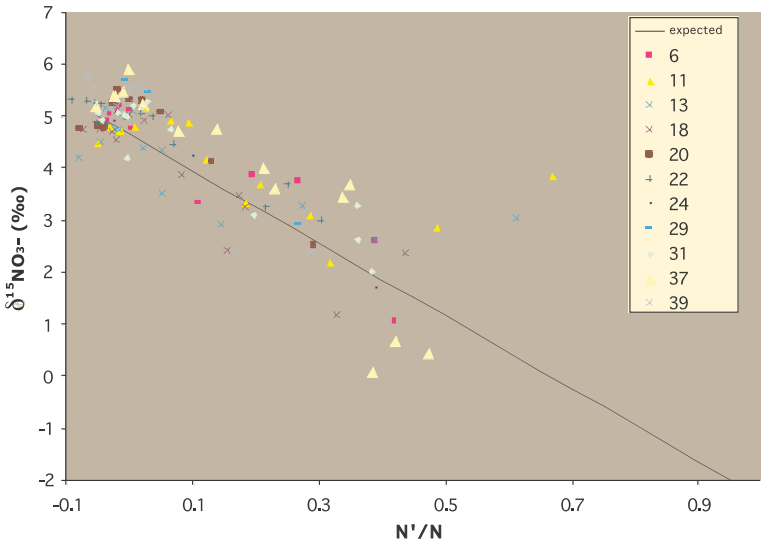

Fig. 3 Cross-plot of the data in Fig. 2. N′ is normalized by the NO_3^- concentration (N′/N) since $\delta^{15}NO_3^-$ should be a function of the proportion of the total derived from N_2 fixation. The *line* represents an expected trend if the newly fixed nitrogen has a $\delta^{15}N$ of – 2‰. *Numbers* refer to the station numbers in Fig. 2

CE a Author: is this change okay?

Editor's or typesetter's annotations (will be removed before the final TEX run)

The principal loci for denitrification in the ocean are regions with suboxic intermediate waters (water column denitrification) and continental margin sediments (sediment denitrification; e.g. [27]). Water column denitrification occurs primarily in three locations; the Arabian Sea [28], the Eastern Tropical N. Pacific (ETNP; [29]) off the western Mexican margin, and the Eastern Tropical S. Pacific (ETSP; [30]) off the Peruvian and northern Chilean margins. In each of these regions, suboxic conditions are vertically found between near the base of the euphotic zone (50 to 100 m) down to as deep as 500 to 1000 m (Fig. 4). Suboxia results from a combination of poor ventilation of intermediate waters and high downward flux of OM. Each of these regions experience coastal upwelling to the surface of nutrient-rich waters which in turn stimulate high rates of primary production. Both upwelling and intermediate water ventilation can be sensitive to climate change suggesting mechanisms for temporal variability in water column denitrification (see below). Although Eq. 10 indicates a build up of NH_4^+ should occur, this is not observed in any of the three water column denitrification regions. An alternative stoichiometry has been used in which organic N as well as NO_3^- is transformed to N_2 and raising its effective yield by 17%;

$$(CH_2O)_{106}(NH_3)_{16}H_3PO_4 + 94.4\,HNO_3 = 106\,CO_2 + 55.2\,N_2 + 177.2\,H_2O + H_3PO_4 \quad (11)$$

NO_2^- is an intermediate for denitrification (see Fig. 1) that can reach substantial concentrations (1 to 10 μM) in subsurface waters as a consequence of intense denitrification. The anammox pathway in which NH_4^+ and NO_2^- are combined to form N_2 by specialized chemosynthetic bacteria has been recently identified and may explain the lack of NH_4^+ buildup [31, 32].

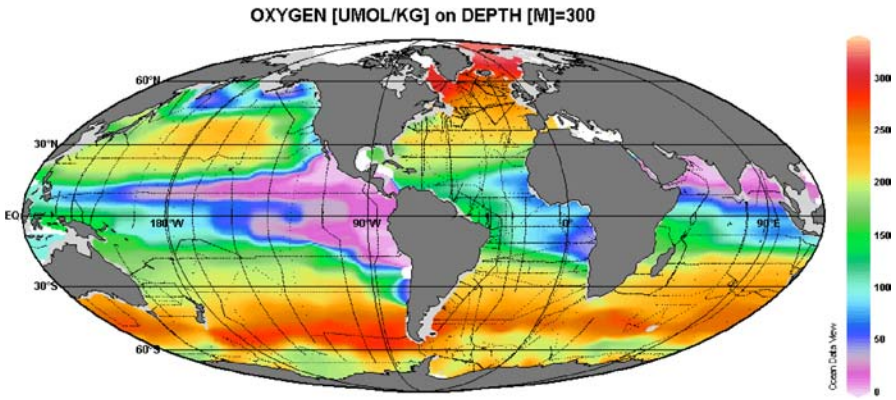

Fig. 4 Global distribution of O_2 at 300 m depth. This depth intersects the cores of the major water column O_2 minimum zones (OMZ's) off the Mexican Margin, the Peru Margin, and in the Arabian Sea

Anammox will be further discussed below. A limited number of measurements of N_2 anomaly relative to changes in NO_3^- have suggested that even Eq. 11 underestimates denitrification yield relative to NO_3^- removal by up to 50% [33].

While only a handful of N_2 measurements of sufficient precision exist for assessing water column denitrification, a relatively large nutrient database exists for calculation of N′. In the case of water column denitrification, the removal of NO_3^- results in negative anomalies relative to PO_4^{-3}. N′ can reach – 20 μM, indicating that up to half of the initial NO_3^- has been removed by denitrification. Just as with N_2 fixation, maps of N′ can provide a detailed picture of the horizontal and vertical extent of the influence of denitrification, if not the active process itself (Fig. 5). Combined with estimates of fluid motion and mixing, a regional denitrification rate can be calculated that is nevertheless dependent on assumptions of stoichiometry (e.g. [12]).

Sediment denitrification is biochemically equivalent to the water column process and occurs in the upper sediment column of inshore regions, the continental shelf, and continental slope. In contrast to water column denitrification, water column O_2 concentrations have secondary influence. Along almost all continental margins, OM inputs are sufficiently high to support respiration rates that result in suboxic conditions. In fact, in margin sediments with the highest denitrification rates, the suboxic zone is found vertically within the sediments as a narrow mm to cm scale band between the oxic sed-

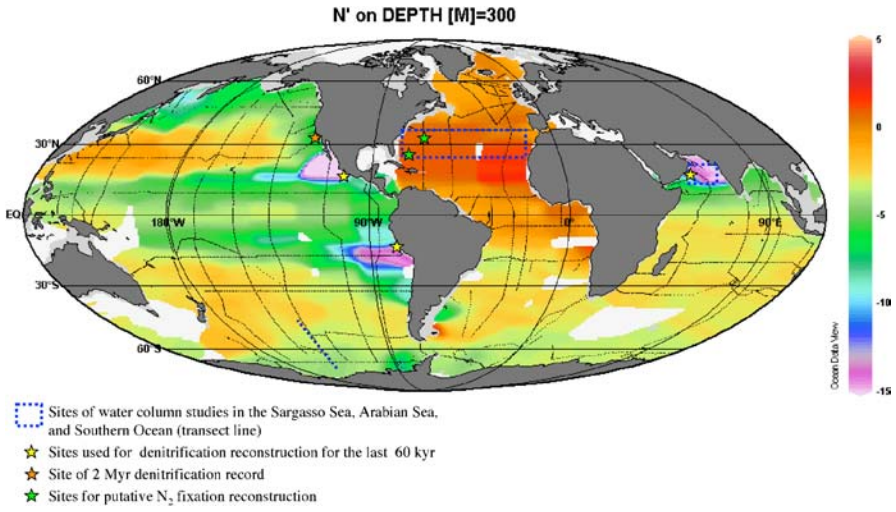

Fig. 5 Global distribution of N′ at 300 m depth. The most negative values correspond to the cores of the OMZ's shown in Fig. 4 and are produced by denitrification. Positive values in the Sargasso Sea and other subtropical zones are the result of N_2 fixation. Site locations for data discussed in this chapter are as indicated

iment surface and an sulfate-reducing, anoxic region below. Until the work of Christensen and Devol [27, 34, 35], the downward diffusion of NO_3^- from the overlying water was thought to control the overall sediment denitrification rate and was used as its estimate. They discovered that in situ production of NO_3^- in the sediment oxic layer by nitrification could be the principal source for denitrification. Their resulting estimates put global marine sediment denitrification on par in importance with respect to water column denitrification ($\sim$ 100 Tg – N/yr). Codispoti et al. [33] and Brandes and Devol [36] have recently suggested even higher rates (> 200 Tg – N/yr). Unfortunately, sediment denitrification estimates are based on extrapolation of flux determinations from a limited number of individual sediment cores from a limited number of regions. This contrasts with water column denitrification in which each major region has been characterized using geochemical estimates.

Unlike N_2 fixation, denitrification strongly discriminates against ^{15}N (large isotope fractionation potential). The two most important implications are (1) locally, denitrification can produce NO_3 strongly enriched in ^{15}N and (2) as an important overall combined sink, denitrification raises oceanic average $\delta^{15}N$ above the average of the combined N sources (discussed further below). Whether measured in the laboratory or in the field, the inherent fractionation factor for denitrification (ε_{den}) is between 20 and 30‰ [37, 43]. The clearest examples of denitrification produced isotope enrichment are for the regions of water column denitrification discussed above. While the oceanic average for $\delta^{15}NO_3^-$ is near 5‰, depths with the greatest intensity of denitrification reach > 20‰. In each of the ocean's three large water column denitrification regions, ^{15}N enrichment in NO_3^- is clearly associated with the core of the O_2 minimum zone (OMZ), and the most negative N′ values. Denitrification also produces $\delta^{18}O$ increases in the residual NO_3^- and recent studies have shown the relationship with the increase in $\delta^{15}N$ is approximately 1 : 1 (D. Sigman, pers. comm.).

N′ can be used to estimate the residual fraction NO_3^- remaining after denitrification permitting fits to the Rayleigh equations (Eqs. 3 and 5):

$$f = (NO_3^- + NO_2^-)/(NO_3^- + NO_2^- - N') \tag{12}$$

Using the Arabian Sea as an example, $\delta^{15}NO_3^-$ maxima within the OMZ vary between stations suggesting variable isotopic fractionation (Fig. 6). Nevertheless, when plotting all station data together, strong linear correlations are found between $\delta^{15}NO_3^-$ and its fractional removal as estimated by Eq. 12, (Fig. 7). Neither the linear fit nor the value for ε_{den} estimated from the slope appears sensitive to the choice of an open or closed system equation. ε_{den} is between 20 and 30‰ consistent with both laboratory and field observations. Similar results have been reported for the ETNP [43].

Although benthic denitrification employs the same biochemical pathways, the measured isotopic fractionation in continental margin sediments is a tenth or less as found in the water column [44, 45]. The cause for this

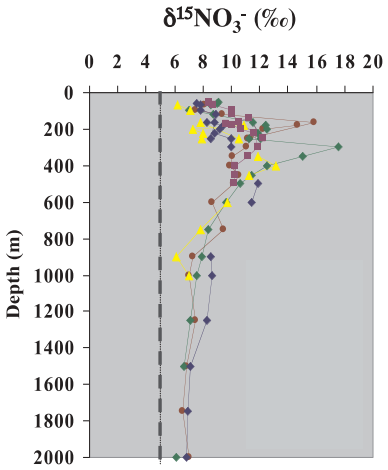

Fig. 6 Depth profiles for $\delta^{15}NO_3^-$ from several stations in the Arabian Sea denitrification zone. The maxima between 200 and 400 m are in the core of this OMZ and co-occur with the most negative N′ values. The *vertical dashed line* represents average oceanic $\delta^{15}NO_3^-$ for reference

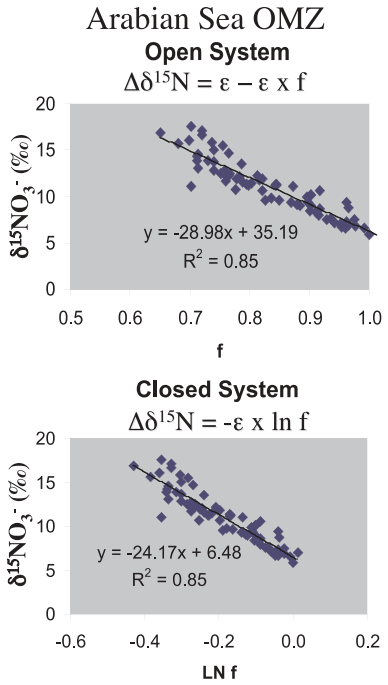

Fig. 7 Cross plots of the $\delta^{15}NO_3^-$ data in Fig. 6 with either the estimated fraction of NO_3^- remaining after denitrification (f) or the ln of f as prescribed by the open and closed system Rayleigh equations (Eqs. 3 and 5), respectively. The regression slopes estimate the fractionation factor (ε)

contrast in ε_{den} between these environments is an apparent distinction in the rate-limiting step. In the case of water column denitrification, the activity of nitrate reductase appears limiting allowing for a near-full expression of the enzymatic fractionation factor. In the case of the benthic denitrification, the sediment matrix impedes the transport of substrates, such that diffusion of NO_3^- is rate limiting. Since this process only very weakly discriminates (fractionates) between isotopes, observed ε_{den} is sharply reduced to values indistinguishable from 0‰.

2.3 Autotrophic Assimilation

While neither a source nor sink to marine combined N inventory, autotrophic assimilation can produce important transient or regional N isotopic signals. Analogous to denitrification, autotrophic consumption tends to discriminate against the heavy isotope such that partial nutrient drawdown leaves the remaining substrate isotopically enriched and the OM produced isotopically depleted. The most important sources of combined N for phytoplankton are NO_3^- and NH_4^+ and significant uptake isotopic effects (ε_u) have been observed during the uptake of either. For NO_3^-, laboratory experiments show ε_u to vary with taxa with some evidence of diatoms having higher values [46–51] as compared with other common marine phytoplankton species.

Aside from eutrophic estuaries/embayments and anoxic basins, NH_4^+ is usually found in the ocean as small, rapidly overturning pools. Any isotopic effects during uptake are not expressed at observable temporal/spatial scales. By contrast, large spatial/temporal variations in NO_3^- concentration are observed in the near-surface ocean which are forced by shifts in the balance between supply and biological consumption. For example, in most temperate oceanic waters, deep winter mixing followed by springtime thermal stratification and a phytoplankton bloom produces an annual cycle of high wintertime NO_3^- followed by springtime drawdown in near-surface waters.

In high-nutrient low chlorophyll regions (HNLC; e.g. Subarctic Pacific, Equatorial Pacific, Southern Ocean), this cycle is muted to varying degrees as a result of Fe limitation of phytoplankton growth (e.g. [52]). In the polar Southern Ocean, summertime NO_3^- drawdown is only between 10 to 20% of the wintertime maximum surface concentration. Northward advection across the polar front into the Subantarctic zone followed by further NO_3^- drawdown produces a large meridional concentration gradient. Since the Subantarctic zone in an important location for intermediate water formation, incomplete nutrient utilization has important consequences for the chemical composition of these waters that ultimately upwell in the subtropics and tropics [53]. A qualitatively similar phenomenon is observed in the Equatorial Pacific where upwelling to the surface of nutrient-rich waters occurs at the equator and more intensely to the east. Here too, Fe limitation prevents

complete local utilization of NO_3^-, but continued utilization with advection of surface waters poleward as well as westward produces a well-known concentration gradient, e.g. [54].

Because these surface NO_3^- gradients are created by phytoplankton drawdown, there are corresponding and inverse variations in the $\delta^{15}NO_3^-$. The best example is from the S. Ocean where near-surface $\delta^{15}NO_3^-$ values can reach 15‰ as $[NO_3^-]$ approaches 0 μM in the vicinity of the subtropical front (Fig. 8; [55]). A Rayleigh-type relationship is observed in all sectors though the estimated value for ε_u (4 to 6‰) may be reduced from actual values due to mixing and seasonal effects. During the JGOFS AESOPS program, there

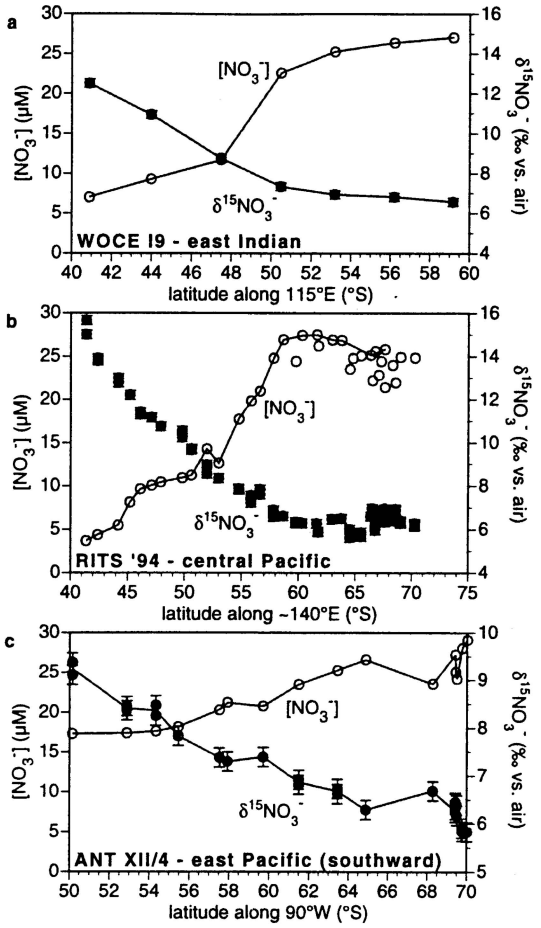

Fig. 8 Changing NO_3^- concentration and $\delta^{15}NO_3^-$ with latitude across the Southern Ocean frontal zone system. Increasing $\delta^{15}N$ with decreasing NO_3^- is the result of isotopic fractionation during phytoplankton uptake. Figure from [55]

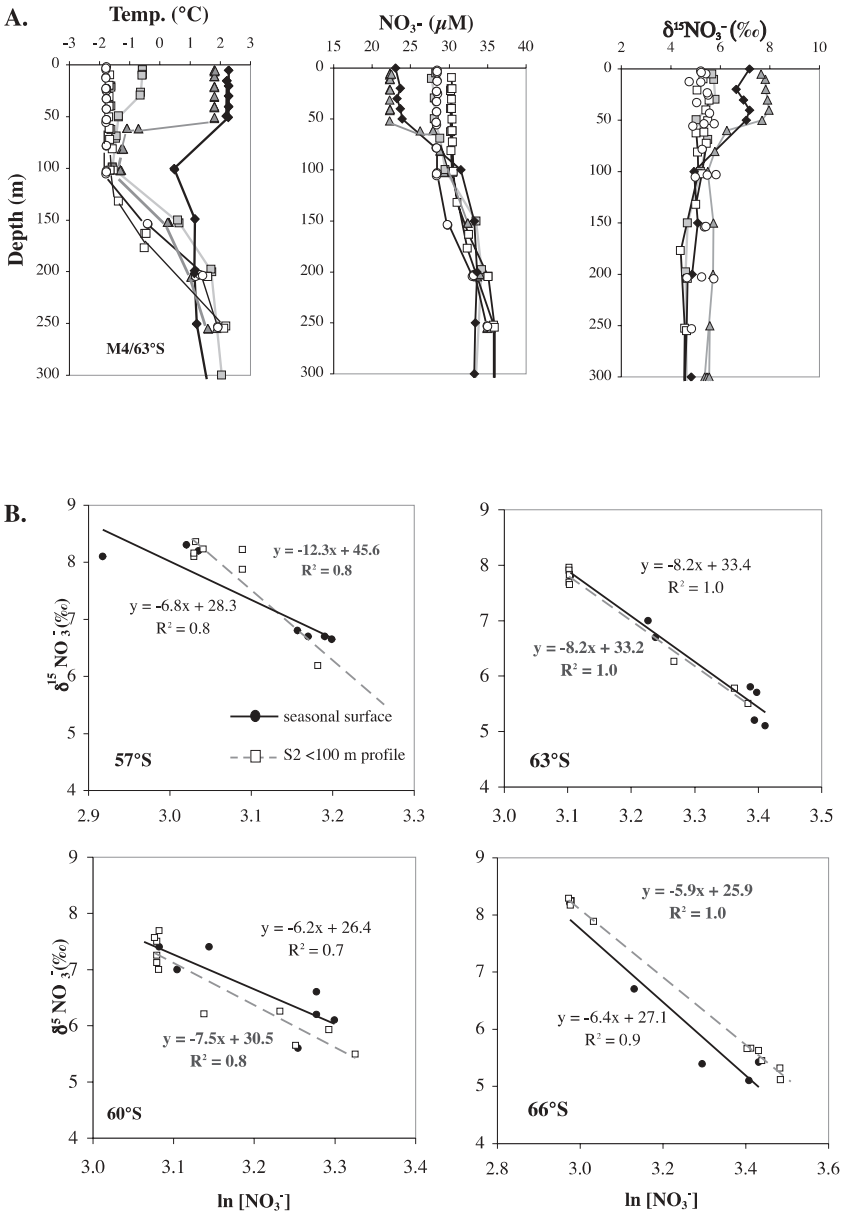

Fig. 9 (**a**) Example of seasonal changes in NO_3^- concentration and $\delta^{15}NO_3^-$ in the near-surface waters of the Southern Ocean due to partial removal by phytoplankton. The corresponding temperature profile marks the progression from well-mixed surface waters in austral winter to thermal stratification in spring. (**b**) Cross plots with ln [NO_3^-], an approximation for ln f, for four stations along a N-S transect of the polar frontal region in the SW Pacific sector. Data from profiles taken at the time of maximal drawdown as well as CE[C] seasonally distributed data are shown

CE[b] Author: is this change correct?
CE[C] Author: is this change correct?

Editor's or typesetter's annotations (will be removed before the final TEX run)

was seasonal sampling at locations within both the subpolar and polar regions north of the Ross Sea. Surface data showed a similar $\delta^{15}NO_3^-$: $[NO_3^-]$ relationship with an obvious seasonal pattern of austral summer reduction in $[NO_3^-]$ and increase in $\delta^{15}NO_3^-$ [56]. Four stations spanning the polar front were studied in detail allowing for more rigorous analysis of quantitative relationships. ε_u was estimated and compared for both summertime vertical profiles of $[NO_3^-]$ and $\delta^{15}NO_3^-$ as well as mixed-layer seasonal time-series (Fig. 9). For both, a similar range in ε_u of 6 to 8 was deduced with the exception of the depth-distributed data at one station. Sediment trap collections at these sites further showed that the annual average $\delta^{15}N$ for sinking POM at each site was consistent with (a) annual NO_3^- drawdown (f) and (b) estimated ε_u. For the low extent of nutrient drawdown observed, it was shown there was insignificant sensitivity to closed (Eq. 4) or open (Eq. 6) system equations. This showed the $\delta^{15}N$ of POM reaching the sediments to be sensitive to surface ocean NO_3^- utilization in HNLC regions.

2.4 Remineralization

Remineralization refers to all processes that transform organic N back into its inorganic constituents. Biochemically this usually involves the heterotrophic removal of the amino group from amino acids with subsequent production of ammonia (NH_3) which at seawater pH is found as ammonium (NH_4^+). While some metazoans subsequently detoxify ammonia by conversion to urea, etc., ammonia is the dominant release product of remineralization in marine systems. The biogeochemical significance of this process is two-fold: First, it is an obligatory step in nitrogen cycling resupplying pools of DIN. Second, it is the "other side of the coin" for organic nitrogen diagenesis—organic nitrogen preservation equates with incomplete remineralization. Conditions that enhance remineralization also enhance diagenesis and reduce preservation.

Evidence for N isotope effects during remineralization is equivocal. Significant isotopic discrimination is indicated by direct observation of low $\delta^{15}N$ for NH_4^+ excreted by zooplankton which is consistent with the well known and ubiquitous phenomenon of ^{15}N trophic enrichment [57–60]. The 3 to 4‰ higher $\delta^{15}N$ for a heterotrophic organism relative to its food is well explained as a mass balance with loss of ^{15}N depleted excreta. The trophic shift in $\delta^{15}N$ has been widely used to trace foodwebs particularly in conjunction with $\delta^{13}C$ which shows a relatively modest change with trophic exchange and is much more indicative of the primary producers at the base of the food web (e.g. C3 vs. C4 plants). Bulk $\delta^{15}N$ has been complemented with individual amino acid isotopic analysis. Large variations within microorganisms have been observed that appear to match position in the transamination pathway [15, 61]. For metazoans which may not have the ability to synthesize all required protein amino acids, the $\delta^{15}N$ of "essential" amino acids appears to retain the

$\delta^{15}N$ of the primary producers while others exhibit an amplified trophic enrichment. Thus, spectra of $\delta^{15}N$ variation among amino acids in zooplankton have been used to deduce trophic level [62].

Additional evidence for isotopic fractionation during remineralization include the universal observation of 5 to 10‰ [63, 64] increases in $\delta^{15}N$ for small, suspended particulate organic matter (POM) with depth below the euphotic zone in the open ocean. With the presumption that deep POM was ultimately derived from the overlying surface waters, the rise in $\delta^{15}N$ with decreasing concentrations was interpreted as reflecting progressive diagenesis with depth and removal of ^{15}N-depleted NH_4^+. Elevated $\delta^{15}N$ (3 to 5‰) for sea floor sediment N relative to sinking particle inputs in regions with poor OM preservation has been interpreted similarly [65].

In contrast, large, fast-sinking POM in the open ocean as sampled by a sediment trap either shows constant or even decreasing $\delta^{15}N$ with depth (1000s of m) and diminishing flux [56, 64–67]. The few direct measurements of porewater NH_4^+ $\delta^{15}N$ show values similar to sediment OM [68]. These measurements were made in the upper 50 cm of relatively OM-rich sediments in regions of the sediment column not influenced by nitrification. It has also been pointed out that even where sediment OM content is relatively high, most of the original input of organic N has been removed by remineralization but nevertheless sediment $\delta^{15}N$ matches well inputs as measured by sediment traps.

Laboratory studies of diagenetic isotopic effects do not resolve these ambiguities. Under oxic and anoxic conditions, $\delta^{15}N$ of the remaining OM can either increase or decrease [47, 69, 70]. These apparently contradictory results may be the result of microbial assimilation of NH_4^+ occurring simultaneously with production. Nevertheless, there appears to be a consensus view that NH_4^+ produced during microbial OM diagenesis is not significantly shifted in $\delta^{15}N$ away from its source [71, 72].

2.5 Nitrification

Nitrification is the last step completing the internal marine N cycle in which NH_4^+ is in two steps oxidized by obligative chemosynthetic bacteria back to NO_3^- (Fig. 1). In the first step, NH_4^+ is oxidized to NO_2^- and in the second NO_2^- is oxidized by a different class of bacteria (e.g. *Nitrobacter*) to NO_3^-. In most of the open ocean, the production of NH_4^+ limits nitrification such that rarely NH_4^+ or NO_2^- concentrations ($< 0.2\ \mu M$) reach significant levels as compared to NO_3^- (1 to 40 μM below the euphotic zone). These intermediaries may build up where nitrification is inhibited by low O_2 as at the boundaries of water column suboxic/anoxic zones or where NH_4^+ production rates are very high such as in eutrophic estuaries.

Laboratory and field studies clearly show a substantial N isotope fractionation effect associated with each of the nitrification steps (15 to 40‰; [73–

75]). The distinction with the diagenesis/remineralization studies is that single strains were used thereby isolating the experiments to single N transformations. New and exciting work shows for the first time variations in ε as a function of phylogenetic grouping presumably due to differences in enzyme structure and/or regulation of microbial physiology [76]. This approach holds much promise for understanding part of the natural variations observed in isotopic fractionation for this and other transformations.

In most of the ocean, nitrification does not produce any observed variation in $\delta^{15}N$ since any remineralized NH_4^+ is rapidly and completely converted to NO_3^-. Only where there is only partial removal or a gradient in utilization in eutrophied coastal waters such as Delaware Bay [74], is there an effect observed through progressive ^{15}N enrichment in NH_4^+ with its consumption by nitrification. A similar effect may occur vertically in OM-rich sediments at the suboxic/oxic transition zone where NH_4^+ is diffusing upward from the anoxic layer and upon entering the near-sediment-surface oxic layer is subject to nitrification [72]. However, if diffusion is rate limiting, little isotopic fraction may occur as observed for sediment denitrification.

N_2O is a by-product of nitrification (Fig. 1) whose yield appears to be dependent on O_2 concentration [77, 78]. Though a very minor sink for combined marine N, this flux may be a large fraction of total global N_2O sources [79, 80]. Atmospheric N_2O acts as a minor greenhouse gas but through photochemical reactions producing NO is a major term controlling stratospheric O_3. The oceanic N cycle through N_2O production thus impacts the chemistry of the upper atmosphere. A number of studies have made use of the $\delta^{15}N$ and $\delta^{18}O$ of N_2O to better constrain its biogeochemistry. Where there is net depletion due to denitrification, ^{15}N and ^{18}O are correspondingly strongly enriched [81]. Recent studies have exploited the asymmetry of the N_2O molecule to examine isotopomer composition, that is the differential $^{15}N/^{14}N$ ratio of the central vs. end position N atom [82, 83].

3
A Geochemical Approach to Marine N Cycling

Availability of combined N is an important control on photosynthetic carbon fixation (primary production) in much of the ocean. Combined N appears to fulfill the definition of a limiting nutrient as first coined by Liebig in his "law of the minimum". Marine biogeochemists have in the last two decades found reality to be rather more complex than this simple view with respect to co-limitation by other macro and micro-nutrients. Moreover, related but distinct processes may have different suites of controlling factors (e.g. primary vs. export production). Nevertheless, it is clear that outside of HNLC regions practically all combined inorganic nitrogen available to the euphotic zone is utilized on an annual basis. This includes regions with perennial coastal

upwelling centers that are persistently enriched near-surface in NO_3^- that is consumed with subsequent along-surface advection of the upwelled water.

As mentioned above, marine phytoplankton produces OM with an average C : N ratio of 6.6 and an average N : P ratio of 17 [10]. This Redfield stoichiometry is a central and powerful concept in marine biogeochemistry and the quantitative link between nitrogen with other elemental cycles. These relationships can be expressed as an equation for the interconversion between average marine OM and its inorganic precursors:

$$(CH_2O)_{106}(NH_3)_{16}H_3PO_4 + 138\,O_2 = 106\,CO_2 + 16\,HNO_3 + H_3PO_4 + 122\,H_2O \quad (13)$$

To the left, OM production consumes NO_3^-, PO_4^{-3}, CO_2, and increases O_2 concentrations in the proportions prescribed. To the right, OM remineralization increases their concentrations by these proportions. An obvious exception is denitrification as discussed above. However, there is still much confusion in the field regarding the precision of the Redfield stoichiometry. A common misperception is that instead of reflecting average behavior, these ratios reflect the strict requirements of all phytoplankton. Therefore, N : P delivery ratios even slightly above 16 would reflect PO_4^{-3} limitation and delivery ratios below N limitation. In reality, there appears to be considerable biological plasticity with respect to nutrient stoichiometry and limitation. Culture and field studies show phytoplankton cell quotas can vary much more dramatically in response to P vs. N limitation (e.g. [84, 85]). This is likely due to the greater structural role that N-containing molecules have. An important confirmation of Redfield's seminal work was the observation that marine phytoplankton, even when nutrients were abundant, utilized NO_3^- and PO_4^{-3} at ratios near 16 : 1. However, more recent work shows considerable variability between taxonomic groups; [86] and that theoretically optimal stoichiometry can vary widely with life strategy [87]. Particularly noteworthy, as mentioned above, is the apparent high N : P ratio, 3 to 4-fold higher than Redfield, for the N_2 fixer *Trichodesmium* [88, 89].

These observations lead to the question of whether available nutrient stoichiometry drives phytoplankton (and OM) elemental ratios or visa versa. Redfield's seminal 1934 paper concluded with the inference that because N sources and sinks were largely controlled by ocean biology whereas P was largely controlled abiologically (source from riverine delivery, sink from sediment burial), the N cycle would adjust to variations in oceanic P balance in order to maintain observed stoichiometry. For example a drop in P delivery would increase N : P, but subsequent inhibition of N_2 fixation would restore it to Redfield values. Since then, many geochemists have viewed P as the ultimate limiting nutrient while biological oceanographers, based on physiological studies, have viewed N as limiting outside of HNLC regions. The observed variability in phytoplankton preferred N : P and in particular

the high N : P (relative to Redfield) of *Trichodesmium* call into question the simplicity of the traditional geochemist's view. As discussed below there is now considerable evidence for past large variations in the ocean N cycle that would have forced fixed N inventory changes independent of P.

Despite these issues, it is clear that there is considerable coupling between oceanic elemental cycles. Of particular interest is the coupling between nutrient and carbon cycles. There is 60-fold more CO_2 dissolved in the ocean than in the atmosphere. It follows that on time-scales of exchange between the atmosphere and ocean ($\sim$ 1000 yr), oceanic processes determine atmospheric CO_2 content which in turn is a major influence on global climate in its role as a greenhouse gas (e.g. [90]). The 40% glacial to interglacial oscillation in atmospheric CO_2 observed in polar ice cores for the last 400 kyr is widely inferred to be driven by oceanic processes [91]. Numerous theories have been proposed over the last 20 years as to which oceanic phenomena produced these changes (see brief review in [53]). Extensive paleoceanographic study has led to many of these being discarded.

The surviving theories include two for which $\delta^{15}N$ data have provided important support. The first theory (or set of theories) focuses on the modern Southern Ocean as the region (1) through which the large volume of abyssal ocean waters is ventilated with the atmosphere and (2) with the largest area of HNLC surface waters [92–94]. Briefly, low glacial CO_2 may have been driven by increased downward export of organic C stimulated by an increase in Fe-rich dust [95]. Alternatively, increased near-surface stratification decreased ventilation of deep CO_2-rich waters. In either case, relative NO_3^- utilization would have increased in glacial polar waters and there is now substantial $\delta^{15}N$ data to support this hypothesis [96, 97]. The second theory involves increased glacial export productivity in all non-HNLC regions due to an increase in average oceanic nutrient concentration. It has been argued from residence time considerations that the response time of the oceanic P inventory is too long relative to the 10 000 yr period for the glacial to interglacial transition in CO_2 concentration [98]. The N residence time is on the order of several thousand years (see below), and is consistent with the oceanic N cycle being able to be perturbed with sufficient rapidity to contribute to the observed change in atmospheric CO_2.

4 Combined N Inventory Balance and Influence on Marine Biogeochemistry

Estimates for annual flux estimates for ocean N sources and sinks have recently been extensively reviewed [33]. The current consensus is that source terms are dominated by oceanic N_2 fixation with significant but more minor contributions from riverine and atmospheric inputs. Denitrification in

the water column as well as continental margin sediments is the predominant sink with very minor contributions from sediment burial. Overall, for a steady state to exist, N_2 fixation must roughly balance denitrification. There are a number of possible feedbacks including the average NO_3^- content of the ocean itself. For example, increasing NO_3^- (excess source over sink) could increase denitrification through increased export productivity and reduced subsurface O_2. Increased average NO_3^- concentration may also inhibit N_2 fixation if subtropical oligotrophy was reduced. Decreasing NO_3^- could produce inverse effects. While such coupling must exist on a very-long time scale, a number of other independent factors can influence either denitrification or N_2 fixation resulting in partial decoupling on climatically significant time scales.

The magnitude of total sources or total sinks are on the order of 200 Tg/yr. Given that the current combined N inventory is 6×10^5 Tg (> 95% in the form of NO_3^-), the residence time (inventory/flux) for combined N in the ocean is about 3 kyr. Any imbalance between sources and sinks would be reflected in a change in inventory on this time scale which is comparable to the time scale for past changes in atmospheric CO_2. By contrast, P residence time is about 5 to 10-fold longer, such that it is much less likely that significant changes in P inventory occurred on deglacial timescales [98]. There is considerable uncertainty, though, in several of the N flux estimates. For example, it was only after integrative, geochemical approaches were taken to quantify average rates of very temporally and spatially variable N_2 fixation that its dominance was recognized as discussed above [11].

While Gruber and Sarmiento [11] assumed that the ocean's N cycle was in rough balance, Codispoti et al. [33] have suggested it is, *at present*, well out of balance by increasing prior estimates of both water column and sediment denitrification to $\sim$ 450 Tg N/yr. The increase in water column denitrification is based on limited data showing the yield of N_2 relative to observed negative NO_3^- anomaly to be up to 4-fold higher than calculated based on Eq. 11. Sediment denitrification was also assumed to be higher than previously thought based on extension of the water column results and recent discovery of anammox and other pathways involving Mn [99].

4.1 What Controls Average Oceanic $\delta^{15}N$?

In parallel with an oceanic N budget, there must also be a ^{15}N budget that controls the average $\delta^{15}N$ of the ocean. If removal processes did not alter (e.g. did not fractionate), nitrogen isotopic ratio then average oceanic $\delta^{15}N$ would simply reflect the weighted average of the sources regardless of the overall magnitude of oceanic N fluxes and whether they were in balance. With N_2 fixation being the dominant term, average $\delta^{15}N$ would be near – 1‰, unless the smaller contributions from riverine and atmospheric inputs are very enriched

or depleted in ^{15}N. In reality, average oceanic $\delta^{15}N$ is near 5‰ [22] and is the result of isotopic fractionation during the predominant sink— denitrification. This value though is well below the one that would be estimated from the known range in ε_{den}; 20 to 30‰ assuming steady state;

$$\mathrm{Flux}_{\mathrm{input}} \times \delta^{15}\mathrm{N}_{\mathrm{avg.\ input}} = \mathrm{Flux}_{\mathrm{denitrification}} \times \delta^{15}\mathrm{N}_{\mathrm{N2\ lost\ via\ denitrification}} \tag{14}$$

since at steady state $\mathrm{Flux}_{\mathrm{input}} = \mathrm{Flux}_{\mathrm{denitrification}}$

$$\delta^{15}\mathrm{N}_{\mathrm{avg.\ input}} = \delta^{15}\mathrm{N}_{\mathrm{N2\ lost\ via\ denitrification}} \tag{15}$$

Eq. 2 applies such that $\delta^{15}\mathrm{N}_{\mathrm{N2\ lost\ via\ denitrification}} = \delta^{15}\mathrm{N}_{\mathrm{avg.\ ocean}} - \varepsilon_{\mathrm{denitrification}}$

$$\delta^{15}\mathrm{N}_{\mathrm{avg.\ input}} = \delta^{15}\mathrm{N}_{\mathrm{avg.\ ocean}} - \varepsilon_{\mathrm{denitrification}} \tag{16}$$

$$\text{or} \quad \delta^{15}\mathrm{N}_{\mathrm{avg.\ ocean}} = \delta^{15}\mathrm{N}_{\mathrm{avg.\ input}} + \varepsilon_{\mathrm{denitirification}}$$

Brandes and Devol [36] have pointed out that lower than expected average $\delta^{15}N$ can be accounted for by the nil effective ε associated with sediment denitrification. Average oceanic $\delta^{15}N$ at steady state is thus largely dependent on the relative contributions of water column and sedimentary denitrification:

$$\begin{aligned}\delta^{15}\mathrm{N}_{\mathrm{avg.\ ocean}} = &\delta^{15}\mathrm{N}_{\mathrm{avg.\ input}} + \mathrm{f}_{\mathrm{wc}} \\ &\times \varepsilon_{\mathrm{wc\ denitirification}} + (1 - \mathrm{f}_{\mathrm{wc}}) \\ &\times \varepsilon_{\mathrm{sed\ denitirification}}\end{aligned} \tag{17}$$

where f_{wc} is the fraction of total denitrification occurring in water column suboxic zones and $1 - f_{wc}$ the fraction in sediments. Considering $\varepsilon_{\mathrm{sed\ denitrification}}$ is close to 0:

$$\delta^{15}\mathrm{N}_{\mathrm{avg.\ ocean}} \sim \delta^{15}\mathrm{N}_{\mathrm{avg.\ input}} + \mathrm{f}_{\mathrm{wc}} \times \varepsilon_{\mathrm{wc\ denitrification}} \tag{18}$$

It had previously been thought that water column and sedimentary denitrification each made roughly equal contributions to oceanic N loss. Brandes and Devol conclude, though, that to achieve an average $\delta^{15}N$ of 5‰, sedimentary denitrification must dominate and account for about 80% of total oceanic denitrification. Since as mentioned above, flux estimates for water column denitrification are likely conservative, the implication is that sedimentary and thus total denitrification is substantially greater than previously thought as concluded by Codispoti et al. (2001). The resulting large imbalance, though, would indicate non-steady $\delta^{15}\mathrm{N}_{\mathrm{avg.\ ocean}}$.

The Brandes and Devol model assumes that use of $\varepsilon_{\mathrm{wc\ denitrification}}$ values derived from cultures and/or from changes $\delta^{15}NO_3^-$ is appropriate for use in Eq. 18. However, there are at least three factors which could reduce the effective isotopic fractionation (difference in $\delta^{15}\mathrm{N}_{\mathrm{N2\ lost\ via\ denitrification}}$ and $\delta^{15}\mathrm{N}_{\mathrm{avg.\ ocean}}$) associated with water column denitrification. The first takes into account that within the water column denitrification zone there is substantial reduction of NO_3^- concentration such that Eq. 4 rather than Eq. 2

would be a more appropriate predictor of the $\delta^{15}N$ of N_2 lost under "closed" system conditions. Using a realistic profile from the Arabian Sea, the effective $\varepsilon_{denitrification}$ is reduced from 25 to 20‰. Second, the canonical denitrification equation shows that 16% of the N_2 produced is actually derived from OM which in water column denitrification regions has a $\delta^{15}N$ between 8 to 10‰ due to the elevated $\delta^{15}N$ of upwelled NO_3^-. The contribution of organic N conversion to N_2 further lowers the effective $\varepsilon_{wc\ denitrification}$ to 16‰. Finally, the nature of the physical flow system also influences effective isotopic fractionation. At one extreme, water parcels can be imagined as being isolated from each other as they pass through (advect) through the denitrification zone and the closed system approach would be most accurate. Alternatively at the other extreme, mixing between parcels greatly exceeds advection and open system assumptions apply. Applying the open system Eq. 6, would further reduce $\varepsilon_{wc\ denitrification}$ to 13‰. Applying all three conditions produces a steady state balance in which denitrification is close to being equally apportioned between water column and sedimentary denitrification (Fig. 10). The lower overall magnitude of sedimentary denitrification called for also makes more likely that a near-steady state in the ocean N budget exists.

The available means to estimate oceanic combined N flux have sufficient inherent uncertainty that the question of modern balance will not be answered through estimation of present-day fluxes. As discussed above, open ocean N_2 fixation is very patchy in time and space though integrative geochemical estimates based on intermediate water NO_3^- anomalies partially overcome this problem. Sedimentary denitrification so far has relied on ex-

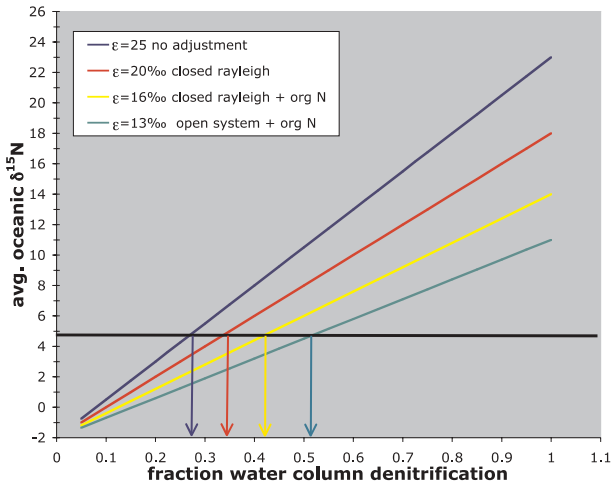

Fig. 10 Estimated relationships between the fraction of total ocean N source consumed by water column denitrification according to Eq. 18. Relationships assuming different values for the effective ε are shown (see text)

trapolation from a limited set of core incubation experiments. However, even if all modern estimates were "perfect" it is unlikely that they would be equivalent to average fluxes over the most recent 3 kyr or approximately 1 N residence time period. It is on this time scale that any net imbalance would have a significant impact on oceanic N inventory. For example, a 20% deficit sustained over the last 3 kyr would roughly result in a 20% decrease in N inventory and average oceanic NO_3^- concentration. Average oceanic $\delta^{15}N$ would similarly respond to unsteady conditions on this time scale. Altabet and Curry [100] showed theoretically that during periods of increasing N inventory $\delta^{15}N$ decreases during the transition regardless of whether the cause is an increase in N_2 fixation or a decrease in denitrification. Decreasing N inventory would correspondingly produce a maximum in $\delta^{15}N$ on the transition. When balance was reestablished, initial average $\delta^{15}N$ would be returned to even though the N inventory was higher or lower unless the relative proportion of sedimentary and water column denitrification had changed. The rest of this chapter focuses on $\delta^{15}N$ reconstruction using sediment cores with application to both the problems of near-modern balance as well as whether changes in N inventory were coupled to past global climate change.

5
Paleo-Reconstruction of Marine N Cycle Processes

5.1
Signal Transfer to and Preservation in Sediments

To use sedimentary $\delta^{15}N$ records for oceanic N cycle reconstruction, it is necessary to (1) understand the factor(s) driving the $\delta^{15}N$ signal reaching the sediments and (2) determine whether that signal is subsequently altered by sedimentary organic matter (SOM) diagenesis.

Dealing first with item #1, it has been long recognized there must be on average a balance in non-HNLC regions between the flux of "new" nitrogen into the euphotic zone where it is utilized by phytoplankton and the loss of N primarily in the form of fast-sinking particles [101]. New nitrogen is distinguished from nitrogen remineralized and reutilized by phytoplankton in the euphotic zone. It is supplied in the form of NO_3^- from deeper waters when they upwell into and/or mix with nutrient-depleted near-surface waters. Just as there is an on average balance between new N input and loss to the oceanic euphotic zone, there must also be an isotopic balance [102]. If so, then the $\delta^{15}N$ signal reaching the sediments as sinking particles should be equivalent to the $\delta^{15}N$ of NO_3^- supplied to the euphotic zone above. In HNLC regions, the same would apply except the $\delta^{15}N$ observed is lowered by the fractionation effect associated with partial NO_3^- utilization as shown by the point for the Equatorial Pacific and Southern Ocean. A priori, this may not be realized

in a $\delta^{15}N$ comparison between NO_3^- and sinking particles if: (1) local vertical processes were not dominant such that balance was only realized by integrating over very large horizontal scales or (2) possible secondary contributors to N loss such as mixing/advection of DON or excretion at depth by vertically migrating zooplankton had large isotope effects associated with them.

Whether sinking particles accurately transfer the NO_3^- isotopic signal to the sediments has been extensively tested by local comparison at a number of sites. At each, in addition to $\delta^{15}NO_3^-$ data, a sediment trap time series was available covering at least one annual cycle. The latter point is important in that many of the locations studied have seasonal increases in euphotic zone NO_3^- due to either seasonal upwelling or wintertime deep convective mixing. Isotopic fractionation due to partial phytoplankton NO_3^- utilization may be expressed on a seasonal basis, but not in the annual average $\delta^{15}N$ for sinking particles since eventually almost all near-surface NO_3^- is utilized at some point in the annual cycle. The sites examined also cover the > 10‰ range in $\delta^{15}N$ observed in the open ocean, from low $\delta^{15}N$ regions influenced by N_2 fixation (Sargasso Sea) to high $\delta^{15}N$, denitrification regions such as the Gulf of California (Fig. 11A). Overall, the comparison is excellent with all points falling on or near the 1 : 1 line. If HNLC regions were included (e.g. Southern Ocean or Equatorial Pacific), these points would fall to the right of the 1 : 1 line in Fig. 11A. In summary, it is clear that local isotopic balance between the new nitrogen source in the form of NO_3^- and loss as sinking particles is realized and that a reliable and well-identified isotopic signature is transferred to the sediments.

This comparison is now extended to the surficial sediments. While the isotopic signature reaching the sediment reflects near-surface processes, early diagenetic alteration may alter it even in recent sediments. Even where sedimentary SOM preservation is considered excellent, only a few percent of the input is preserved. While the isotopic effects of diagenesis *per se* remain ambiguous, SOM may also have altered $\delta^{15}N$ relative to inputs if bacterial metabolism produces new organic nitrogen from NH_4^+ or NO_3^- with $\delta^{15}N$ distinct from sinking particles. The comparison with surficial sediment $\delta^{15}N$, though, shows these concerns are not actualized when SOM preservation is good to excellent. For these sites in which %N in surficial sediment is relatively high (> 0.1% by weight) as a result of a combination of high export production and/or inhibited diagenesis resulting from low bottom water O_2, the 1 : 1 comparison between SOM $\delta^{15}N$ and $\delta^{15}NO_3^-$ is just as robust if not more so as between $\delta^{15}NO_3^-$ and sinking particle $\delta^{15}N$ (Fig. 11B). In contrast, deep-ocean sites such as the Sargasso Sea with poor SOM preservation have $\delta^{15}N$ values elevated by 3–6‰ relative to sinking particles. This "diagenetic effect" is clearly qualitatively linked to reduced preservation in bottom environments that receive less OM input, have high O_2, are well bioturbated, and have lower sediment accumulation rates. However, the mechanisms producing this effect are equally unknown as for the ^{15}N enrichment of deep,

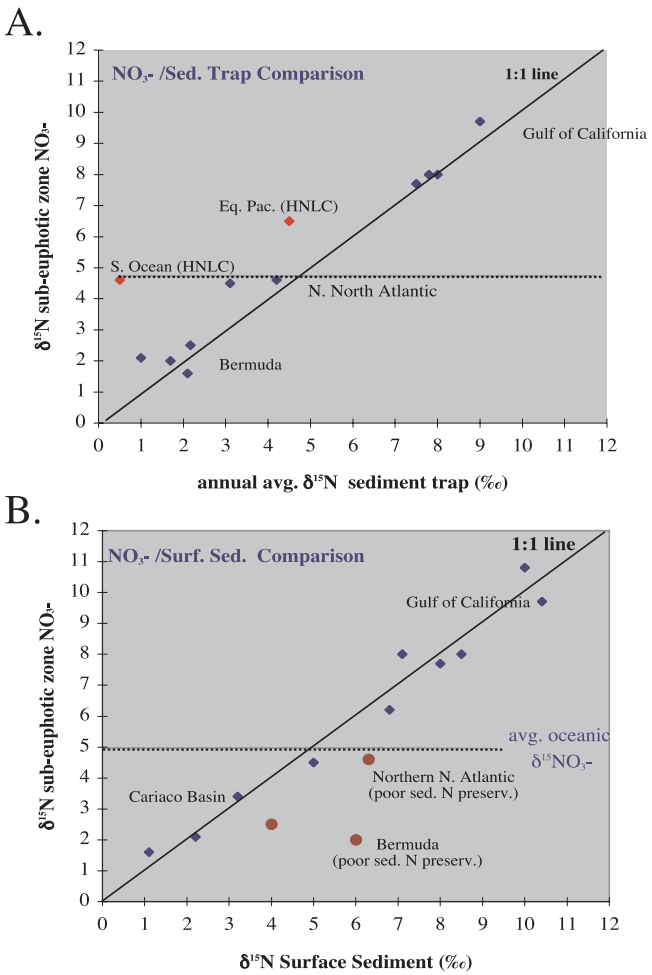

Fig. 11 **A** Sub-euphotic zone $\delta^{15}NO_3^-$ vs. annual average $\delta^{15}N$ for sinking particle sampled by sediment trap. **B** Sub-euphotic zone $\delta^{15}NO_3^-$ vs. surface sediment $\delta^{15}N$. For both panels, a 1 : 1 line as well as a *horizontal dashed line* representing the oceanic average $\delta^{15}NO_3^-$ are shown for reference. Note the departure from the 1 : 1 *line in panel B* for sediments with poor N preservation. Data sources other than those already cited are found in [127–142]

suspended particles. While it may be tempting to assume that the diagenetic increase in $\delta^{15}N$ is constant downcore at any particular site, we have no means so far to independently determine this.

Reliable and detailed $\delta^{15}N$ paleo-reconstructions are thus, to date, restricted to sediments with good to excellent preservation of OM with one important exception. In the polar Southern Ocean, sediments are typically rich in biogenic opal consisting primarily of diatom frustule microfossils. Like all or-

ganisms which produce biominerals, diatoms use organic templates to direct their growth which are then permanently incorporated in the mineral matrix. The organic template with a typically high protein content is relatively protected from diagenetic alteration after the organism's death. Biogenic opal has a number of advantages as a reservoir of protected OM in the sediments. It has significantly lower density that the other major components of deep-sea marine sediments, clays and calcites, such that it can be readily separated using density centrifugations. Its chemical resistance permits the use of strong oxidants such as hot perchloric acid for rigorous surface cleaning of extraneous OM. Sigman et al. [97] showed that lowered apparent N content from cleaned diatom frustules corresponded to lower δ^{15}N and a less "noisy" downcore record. As discussed above past changes in δ^{15}N in the Southern Ocean are most likely associated with changes in NO_3^- drawdown by phytoplankton and results to date indicate greater drawdown of near-surface NO_3^- in the polar Southern Ocean during the last glacial period [97, 103]. Recently it has been shown, though, that the presence of atmospheric N_2 "dissolved" in frustules may pose a contamination artifact that would bias δ^{15}N results [143], (Altabet unpublished). Potentially other biominerals may be exploited as repositories of unaltered OM for isotopic reconstruction and there has been continued effort to make use of the preserved calcite tests of foraminifera [100] and coccoliths produced by coccolithophorids.

Isolation of specific biomarker molecules from sediments for C and H isotope analysis has proven very successful in both avoiding the effects of diagenesis and to isolate the source of the isotopic signature. In contrast, there has been comparatively little progress in N-specific biomarker isotope analysis. The reasons for this are both technical and phenomenological. N is found in much lower abundance in molecules as compared to C and H requiring much larger quantities to be extracted and purified. N-containing biomarker molecules are also typically more polar and less volatile (e.g. peptides and amino acids) making them more difficult to purify and separate using now standard GC interfaces to isotope ratio mass spectrometers (IRMS). Extra care in the GC-IRMS interface needs to be taken to ensure that N_2 is the only product of combustion (no N oxides) and that there is no contamination from atmospheric leaks. Additionally, common N-containing biomarkers are not specific; all organisms produce amino acids and nucleic acids. An important exception is chlorophyll and its derivatives (chlorins) which are produced only by photosynthetic organisms and contain 4 N atoms per molecule. Despite the difficulties of off-line preparation of sufficient material for isotopic analysis, δ^{15}N chlorin data have been used to show that the relatively high δ^{15}N of Mediterranean low OM sediment sequences is largely due to diagenesis [104, 105]. Efforts to develop a GC-IRMS technique for these low volatility molecules have to date not been successful. Neither have amino acid δ^{15}N analysis been applied to sediments, though their organic geochemistry in recent sediments has been examined using δ^{13}C [106].

5.2 Reconstruction of Water Column Denitrification

The most successful application of downcore $\delta^{15}N$ reconstruction has been in identifying and understanding past changes in water column denitrification on time scales from 10^2 to 10^6 years. Water column denitrification is regionally isolatable, produces large isotopic signals as shown above, and is strongly coupled to past climate change. Suboxic intermediate waters overlying margin sediments with high OM input ensure both fidelity of the preserved $\delta^{15}N$ signal and the availability of cores with high accumulation rates for good to excellent temporal resolution. In these sediments, N content is high enough that only ten's of mg of material are necessary for isotopic analysis. Reconstruction of other marine biogeochemical processes such as near-surface nutrient utilization have been made, but instead of a broad review, we focus here on denitrification for detailed illustration.

Detailed denitrification records based on sediment $\delta^{15}N$ have been published for the Arabian Sea [42, 107, 108] and the ETNP [109–111]. In the latter case, sites along the western American margin are included since upwelled waters are derived from the California Undercurrent which in turn carries denitrification-influenced water northward from the ETNP. Current studies now also include the Peru Margin (Higginson et al., submitted), the third of the ocean's major water column denitrification zones.

Variation in Arabian Sea denitrification occurs on a variety of climatologically relevant time scales. The longest record from the Owen Ridge off Oman reaches back nearly 1 Myr from the present [42]. Variation is primarily at the Milankovitch periods of Earth' orbital variation (23, 41, and 100 kyr) which are also found in the glacial cycles of Pleistocene climate. In general, lower $\delta^{15}N$ and denitrification is found during cold periods of glacial maxima. Nearby cores from the Oman Margin have 10-fold higher accumulation rates and provide better temporal resolution (Fig. 12). A detailed study of the last 60 kyr at centennial resolution reveals strong millennial variability during MIS 3 (30 to 60 kyr BP), with transitions from low $\delta^{15}N$ to $\delta^{15}N$ maximum occurring relatively abruptly, on the order of a few hundred years or less [108]. The pattern of variation over this period is remarkably similar to temperature changes recorded in Greenland ice cores and known as Dansgaard–Oeschger events after their discoverers (e.g. [112]). Again, cold events are associated with $\delta^{15}N$ minima and visa versa. It is apparent that broad-scale (perhaps global), rapid climate is strongly coupled to Arabian Sea denitrification intensity.

We can make use of nature's "past experiments" to probe the causes of changing denitrification intensity by analysis of synoptic proxies of relevant processes. A leading hypothesis linking N. Hemisphere climate to Arabian Sea denitrification is that climate change modulates the strength of the summer South Asian monsoon and upwelling favorable winds off Oman. Correspond-

ing oscillation in productivity influences subsurface suboxia and thus denitrification intensity in the Arabian Sea. Consistent with this hypothesis, a site on the nearby Owen Ridge has records for wind strength (sediment grain size) and productivity (%N) which are positively correlated with δ ^{15}N at the orbital periodicities. For the Oman Margin sites, further support is found in positive relationships between δ^{15}N, %N, and chlorin concentration.

The high accumulation rate of ODP site 723 (15 cm/kyr) and the low material requirements for key analyses permit an extremely well-resolved exploration of the relationship between climate-linked of[CE d] denitrification and its putative proximal forcings (Higginson et al., in press[TS e] GCA). A 20 cm

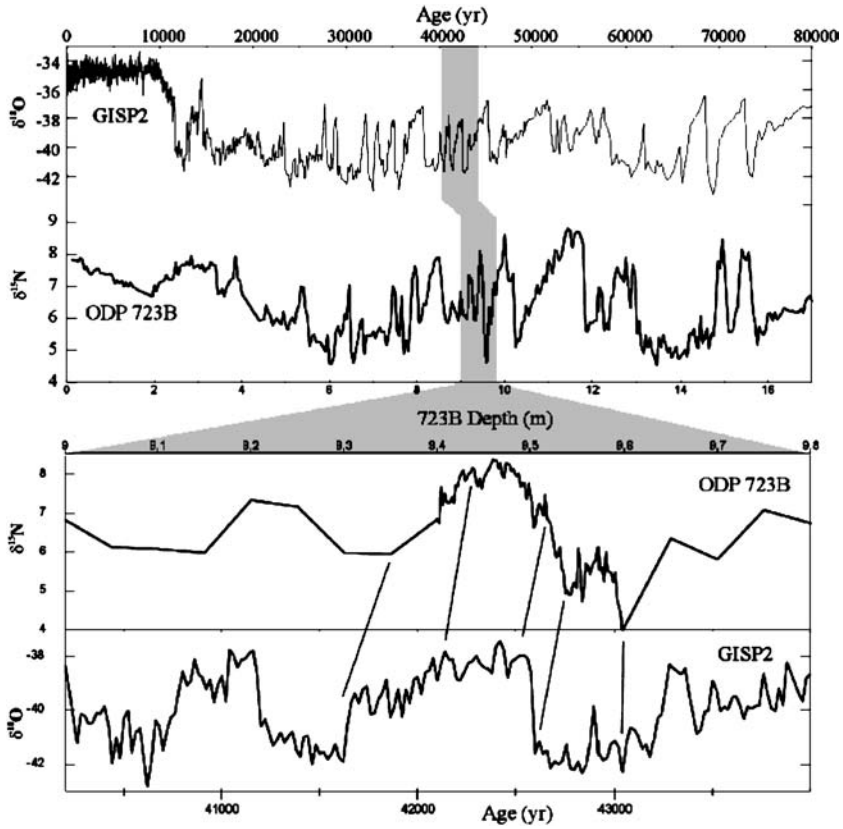

Fig. 12 *Upper Panel.* Comparison between Greenland ice core record of climate (ice δ^{18}O reflects local temperature) over the last 80 kyr and Arabian Sea denitrification (δ^{15}N). ODP Site 723B is located on the Oman Margin at about 800 m depth at the lower boundary of the OMZ. MIS 3 is the period between 30 and 60 kyr before present and the sub-millennial scale rapid D-O events are reflected in both records. *Lower Panel.* The approximate 1 kyr period examined at very high temporal resolution through 2 mm sectioning of the sediment core. This section corresponds to D-O event #11

[CE d] Author: do you mean 'to'?
[TS e] please update, if possible

Editor's or typesetter's annotations (will be removed before the final TEX run)

section of ODP Site 723A corresponding to the D-O event #11 was sectioned at 2 mm intervals to achieve decadal resolution (Fig. 12). $\delta^{15}N$ results show a very well-resolved transition over 100 to 200 years from little or no denitrification during the cold-stadial period to near-maximal denitrification during the warm, interstadial period. At the point of this transition, there is a simultaneous rise in productivity proxies; OM accumulation and Ba (Fig. 13). Higher export productivity and therefore increased OM transport to the sediments should result in higher sediment respiration as confirmed by reduced $CaCO_3$ preservation. For productivity to force denitrification, it must produce suboxia in intermediate waters. Low O_2 is known to increase V and Mo and reduce Mn in sediments (e.g. [113]). These changes are also observed coincident with the increase in productivity and denitrification (Fig. 13). Other sed-

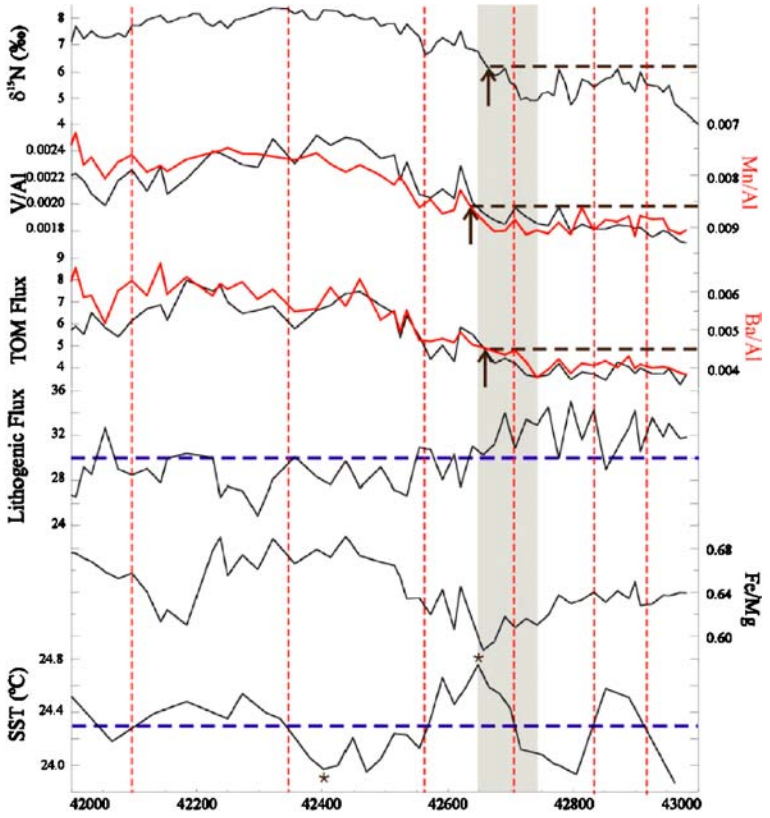

Fig. 13 Multi-proxy, very high resolution reconstruction of D-O event #11 from ODP Site 723B in the Arabian Sea. The increase in denitrification starting about 42 700 yrs bp is accompanied by decreased oxygenation of the overlying water column (V/Al increases, Mn/Al decreases) and increased productivity (increasing Ba/Al and TOM flux). Changing Fe/Mg also marks changing terrestrial aridity in eolian dust source regions

iment proxies can be exploited to probe the cause and effect linkages between climate change and marine biogeochemical processes such as denitrification. One example is dust-born proxies for terrestrial conditions transported by winds to the study region. Here the Fe/Mg ratio varies such that the stadial period of low Arabian Sea denitrification is also marked by more arid conditions on nearby continental land masses. The strength of the S. Asian monsoon may be modulated at these suborbital timescales by changes in land cover and corresponding ability to absorb sunlight.

In sum, intermediate water suboxia and denitrification are regionally forced by changes in southern Asia monsoon intensity. It is likely that productivity and subsurface respiration are the linking processes. While remote changes in water mass ventilation can be ruled out, coincident changes in local ventilation of intermediate waters cannot, without studies of past changes in the hydrography of these waters.

Studies in the ETNP have shown similar linkages between past-climate change and denitrification with glacial periods marked by lowered levels. To date there is no evidence of D-O event forcing as strong as observed in the Arabian Sea. This observation is likely related to the greater potential for remote forcing of ventilation in this eastern boundary current. It has been argued that coincidence with productivity proxies demonstrates local forcing of suboxia and denitrification [109]. More recent work indicates significant phase lags between the two [111]. It has also been argued that changes in the proportion and ventilation of the source of intermediate water in the ETNP is the major proximal control on ETNP intermediate water oxygenation [114]. One source is "old" equatorial underwater which is remotely ventilated in the Southern Ocean. Another is Pacific Intermediate Water ventilated in the Subarctic NW Pacific. If true, denitrification in the ETNP could be modulated principally by high latitude processes as opposed to proximal subtropical processes as in the Arabian Sea.

We have examined denitrification variations for nearly the last 2 Myr years from ODP Site 1012 at the northern boundary of the ETNP (Fig. 14). The significance of this portion of the latest Pleistocene is that it encompasses the mid-Pleistocene transition from 41-kyr period dominance to 100-kyr dominance in glacial/interglacial variations. The cause of this transition is the subject of intensive research particularly since the 100 kyr period is the weakest with respect to solar forcing despite its dominance over the latest 0.5 Myr (e.g. [115]). Our data show large variations in δ^{15}N and denitrification throughout this time period with no long-term trend. Spectral analysis demonstrates the importance of the 100, 41, and 23 kyr periods over the last 0.6 Myr (Fig. 14 inset). However the earliest 0.6 Myr shows no significant 100 kyr periodicity but a strong 41 kyr period along with a harmonic near double this period. Clearly the climate-denitrification link extends to these Myr timescales.

The Peru Margin is the third and last of the major water column denitrification regions to be subjected to paleoceanographic reconstruction. A priori

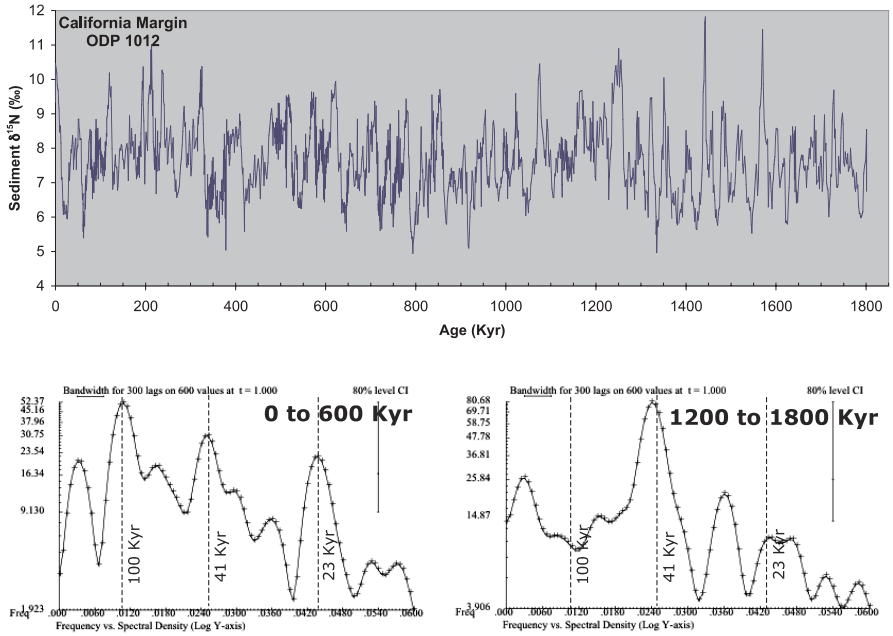

Fig. 14 Denitrification record for the ETNP over the last 1.8 Myr. ODP site 1012 is located on the southern California margin. Though this site is not properly within the ETNP, a coastal undercurrent that is the source of upwelled waters carries NO_3^- whose isotopic composition is influenced by ETNP denitrification. The inset shows spectral analysis results showing the change in major mode of variability from 41 to 100 kyr bp at the mid-Pleistocene transition about 600 kyr ago

we may expect differences in climate response as compared to the Arabian Sea and ETNP since this region is only one of the three located in the Southern Hemisphere. As elsewhere, margin sediments overlaid by low O_2 present the best targets due to excellent OM preservation and high accumulation. As in the ETNP, laminations and banding are indicative of periods of sufficiently low O_2 to exclude bioturbating organisms and present the potential for ultra-high temporal resolution studies. However, the Peru margin has presented a number of challenges for paleoceanographic research, the foremost of which are (1) difficulties in dating and age model construction due to paucity of foram tests preserved in the sediments and (2) the presence of hiatuses in most cores marked by phosphorite and/or course grain layers. We have largely overcome these problems by employing for nearby Peru margin sites an innovative dating technique based on ^{14}C dating of extracted and purified algal biomarker compounds [116]. While no single core available to us continuously spans the last 20 ka, the regional nature of the $\delta^{15}N$ signal allows for overlapping sections to be correlated to produce a composite $\delta^{15}N$ record (Fig. 15). The chronology of the composite high-resolution $\delta^{15}N$

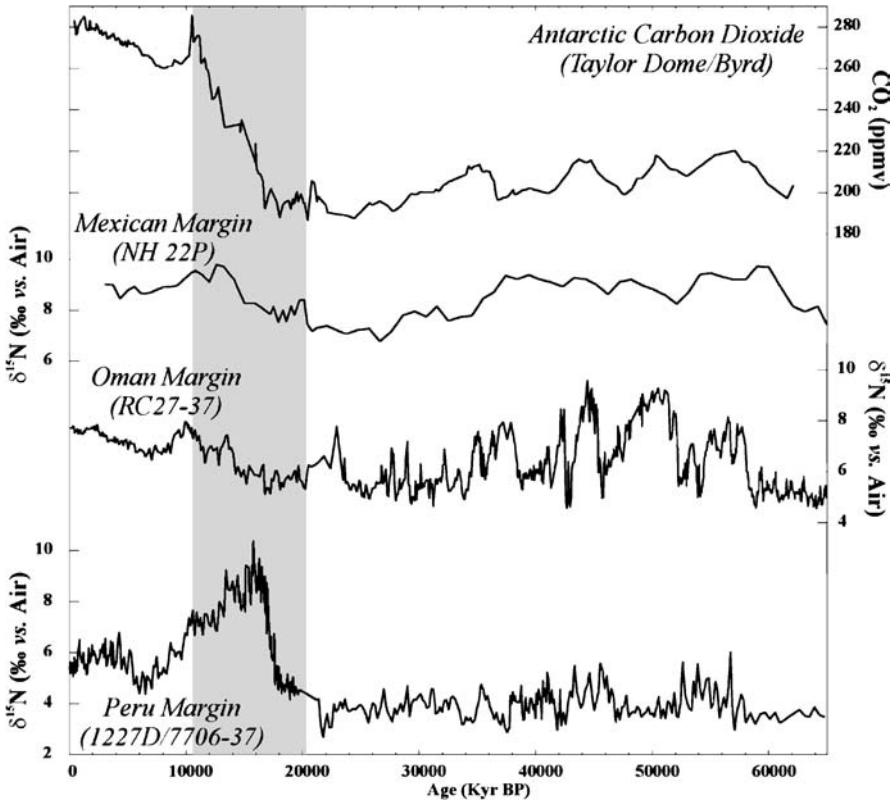

Fig. 15 Comparison of δ^{15}N records from the three major water column denitrification zones covering the last 60 kyr. Note the relatively low δ^{15}N values and absence of D-O events for the Peru Margin record during MIS 3 (30 to 60 ka bp) and the early and sharp rise during the early part of the last deglacial period (14 to 18 ka bp). The ice core record for atmospheric CO_2 is shown for [144]. The Mexican Margin data is from [109] and the Oman Margin data is from [108]

record is verified by comparison with a low-temporal resolution record from a low accumulation rate core from off margin with conventional dating based on foraminiferal ^{14}C and δ^{18}O. We have extrapolated our chronology beyond our last dated interval near 25 ka to give a 1st order view of MIS 3 (25 to 60 ka before present).

Not surprisingly, large variations in δ^{15}N and hence denitrification are observed over the last 50 ka. As in the Arabian Sea and ETNP, upon deglaciation there is a dramatic ramp up in denitrification. However, the history of Peru denitrification departs from its northern hemisphere counterparts in several striking respects. First, the deglacial peak in denitrification occurs very early at between 15 and 16 ka, when most of the planet was still very much experiencing glacial conditions. We suspect that this is the result of Southern

Hemisphere forcing of intermediate water ventilation. An important source for the intermediate waters of the Peru OMZ is Subantarctic Mode Water (SAMW) which is formed in the Subantarctic section of the Southern Ocean and a number a climate records from this and the polar region even further to the south suggest early initiation of the deglacial sequence (e.g. [117]). Second, MIS 3 (30 to 60 ka) shows overall low denitrification similar to LGM levels except for modest maxima that may be related to Antarctic Climate Events (ACE's) as observed in Antarctic ice cores. This again is in contrast to the Northern Hemisphere records which show near-Holocene values with D-O event variability further supporting distinct Southern Hemisphere forcing. Third, there is substantial late Holocene variability in denitrification with excursions in $\delta^{15}N$ almost as large as upon deglaciation occurring over centuries or less. Of the three denitrification regions, Peru is most impacted by ENSO (El Niño/La Niña) variability, and while individual ENSO events cannot be observed at our temporal resolution, changes in the overall frequency and amplitude would be. During El Niño, isopycnal surfaces are depressed off Peru such that upwelling brings nutrient-poorer water to the surface with lowered productivity and the OMZ resides more deeply. It would thus be expected that sinking particles would have reduced $\delta^{15}N$ during El Niño events, and the minima in the late Holocene record may correspond to periods where these are more frequent and more intense.

5.3 A Composite Denitrification Record

With good to high quality $\delta^{15}N$ records now available from each of the major water column denitrification zones, a first attempt can be made to assess the combined influence of these regions over the last 60 kyr. This is done by first normalizing the variability in each record selected about its average value and producing a 3-kyr smoothed composite of the three assuming each contributes one third of total water column denitrification for the time period considered. The result is found in Fig. 16 which shows low overall denitrification in MIS 3 and the LGM, a rapid rise to high late deglaciation and early Holocene values, and moderate levels during the mid- and late Holocene. When compared to atmospheric CO_2 as observed in ice cores, there are striking similarities including the 4 maxima of moderate intensity during MIS 3. Importantly, the deglacial rise in denitrification leads CO_2 by the approximate residence time for combined N in the ocean. That is, if changing denitrification is influencing atmospheric CO_2, it would do so by changing the oceanic N inventory with a lag on the order of its residence time of about 3 kyr.

The changes in water column denitrification described were proximally forced by changes in the intensity and extent of OMZ's. OMZ modulation in turn was forced by changes in organic carbon flux and/or intermediate water ventilation and there has been discussion in the literature of the sen-

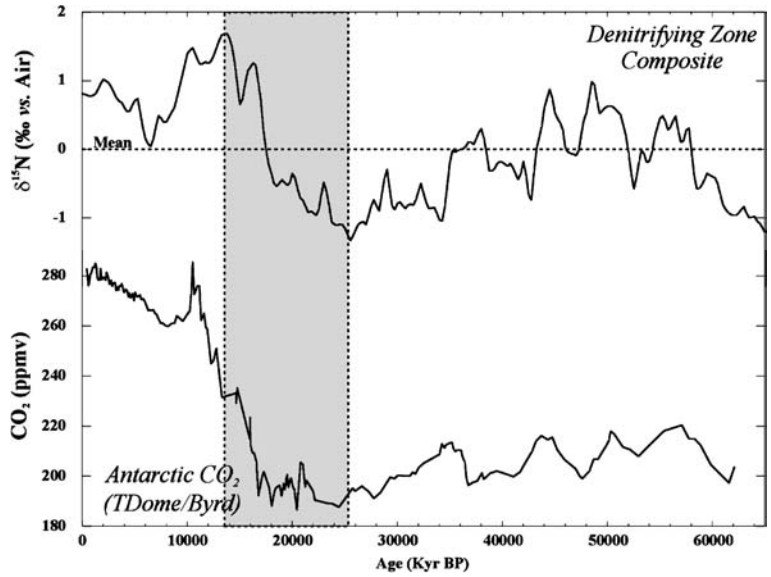

Fig. 16 Comparison of global CO_2 record [144] and composite global water column denitrification record. (see text for details)

sitivities of these to climate change phenomenon. Another consequence of OMZ modulation is likely change in oceanic N_2O flux to the atmosphere. As mentioned above, N_2O is an intermediate in the denitrification pathway as well as a by-product of nitrification. Its yield relative to NO_3^- production is negatively correlated with O_2 concentration such that the highest oceanic N_2O concentrations are found in oceanic OMZ's prior to the onset of denitrification [118]. It has been hypothesized that expansion/contraction of oceanic OMZ's would also correspond to changes in oceanic N_2O flux to the atmosphere. A correlation between atmospheric N_2O as recorded in ice cores and Arabian Sea denitrification has been cited as evidence [119]. N_2O also acts as a powerful greenhouse gas and would add to the proposed climate change effect from CO_2 changes brought about by changes in oceanic N inventory.

5.4 Toward Reconstruction of the Complete Oceanic N Budget

Sediment $\delta^{15}N$ records from the three water column denitrification zones have provided well-resolved histories for each of these regions. Though important, they still provide only an incomplete understanding of both past changes in marine N cycle and its modern dynamics. A wish list in this respect would include reconstruction of sedimentary denitrification, N_2 fixation, and average state of the marine N cycle.

Unfortunately, it is unlikely that $\delta^{15}N$ can be used to directly reconstruct sediment denitrification. It leaves little or know isotopic imprint on oceanic $\delta^{15}NO_3^-$ and it is widely distributed throughout all sediments with suboxic layers, particularly along continental margins. There is also no evidence for sedimentary denitrification influencing the $\delta^{15}N$ of sedimentary organic N which is the source for coupled nitrification–denitrification. Fortunately, inability to reconstruct sedimentary denitrification does not eliminate any hope of sufficiently complete marine N cycle reconstructions. Knowing water column denitrification, N_2 fixation, as well as relative changes in N inventory would be sufficient for this.

Any thorough reconstruction of the ocean's N cycle, though, does require assessment of any past changes in N_2 fixation. Just as denitrification imparts a regional "heavy" N isotopic signature to subsurface NO_3^- and ultimately to the underlying sediments, N_2 fixation should impart a "light" isotopic signature to the sediments below. Above, we showed evidence for the modern ocean of decreased $\delta^{15}NO_3^-$ which in turn influences the $\delta^{15}N$ of sinking particles. Unlike denitrification zones, N_2 fixation is found principally in oligotrophic subtropical gyres where the underlying sediments typically have poorly preserved OM as a result of low OM flux, great depth, and high bottom water O_2. Accordingly, sediment $\delta^{15}N$ has been modified upward by diagenesis. While $\delta^{15}N$ records of modest temporal resolution can be obtained in regions such as the Sargasso Sea (Fig. 17), we have little confidence in assuming the upward diagenetic shift has been constant over time. Nevertheless, the lower $\delta^{15}N$ values during the LGM suggest that N_2 fixation did not decrease to compensate for reduced denitrification. In fact, the broad features in this record are seen in a number of records from outside of both denitrifying and HNLC zones suggesting that a global response is recorded instead of local changes.

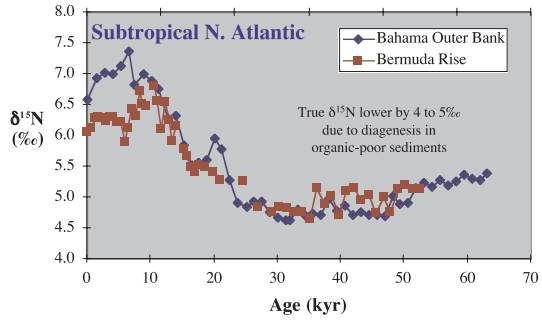

Fig. 17 Sediment $\delta^{15}N$ records from two locations in the Sargasso Sea. Organic N is only poorly preserved at these deep-sea, oligotrophic sites and $\delta^{15}N$ values are shifted upward by 4 to 6‰ from the primary signal. Nevertheless, the observation of lower glacial values is indicative that N_2 fixation in this region was not lower than at present

There are a number of avenues to overcome the diagenetic problem in N_2 fixation as well as other regions with poor sedimentary OM preservation. Just as in the Southern Ocean diatom microfossils were exploited as reservoirs of preserved OM [97], calcareous microfossils which are more abundant in N_2 fixation regions may prove to have similar utility. Assessments of diagenetic state independent of $\delta^{15}N$ may be used to "correct" downcore $\delta^{15}N$ data for variations in diagenetic influence.

5.5 Oceanic Wide Changes in $\delta^{15}N$ Revisited

Due to good OM preservation and not being located in either an HNLC nor denitrification region, sediment records for $\delta^{15}N$ from the South China Sea have been cited as evidence for little change in ocean average $\delta^{15}N$ over the last glacial cycle [120]. This has led to the conclusion that either N_2 fixation changes compensated for any change in denitrification and/or there was no change in the proportioning of denitrification between the sediment and the water column [36]. However, subsequent work in this area has shown that significant variations occurred in a nearby site and assigned them to possible changes in water mass source due to sea level change [121]. Another approach is to consider all available records from regions that are neither directly influenced by water column denitrification nor are within HNLC regions regardless of OM preservation to detect common trends (Table 1). While each of these records could individually be questioned as to the influence of local processes or diagenesis, in aggregate a consistent picture is apparent in which there is a 2 to 3‰ increase in $\delta^{15}N$ from the LGM to early Holocene and a subsequent 1 to 2‰ decrease to the present. Qualitatively, this supports a global oceanic impact from changes in water column denitrification; increasing (as a fraction of N_2 fixation) upon deglaciation with subsequent decrease perhaps due to a "slow" feedback mechanism. If Fig. 10 is used to estimate the magnitude of these changes, water column denitrification as a portion of the total N flux varied by up to $\pm$15% between the LGM and present. Alternatively, N_2 fixation could have decreased upon deglaciation but this scenario is not supported by any of the water column denitrification records nor the putative $\delta^{15}N$ record from the Sargasso Sea (Fig. 17). These changes would have resulted in significant variations in oceanic combined N inventory. For example a 15% increase in denitrification relative to N_2 fixation over 5 kyr would decrease total ocean inventory by about 25%. Of course, this perspective assumes no insidious compensation by opposite and equal changes in sedimentary denitrification. In fact, it has been argued that sedimentary denitrification would only have increased upon deglaciation and the increased shelf sediment rise produced by sea level rise [27]. As discussed above, the major parameters needed for near complete reconstruction of past variations in the oceanic N budget are potentially obtainable.

Table 1 Summary of $\delta^{15}N$(‰) changes at oceanic sites which are neither within HNLC or denitrifying regions. Overall these results are indicative of change in global average marine $\delta^{15}N$. *Upper panel* from sites with a relatively high sediment accumulation rate (> 10 cm/kyr) and good N preservation. The *bottom panel* for sites with a low accumulation rate (< 5 cm/kyr) and sufficiently poor N preservation that diagenetic effects are apparent. Early to late Holocene refers to the period from approximately 10 ka b.p. to present. LGM (last glacial maximum) to early Holocene refers to the period from 20 to 10 kyr b.p.

High-resolution, good N preservation sites	Early to Late Holocene
Cariaco Basin *	– 3
S. China Sea [121]	– 1
Gulf of Maine *	– 2
Delmarva Slope *	– 0.8
Carolina Slope *	– 2

Low-resolution, poor N preservation sites	Early to Late Holocene	LGM to Early Holocene
Bermuda Rise +	– 1	2.5
Bahama Outer Bank +	– 1	3
Benguela [122]	– 0.5	2
Arctic Ocean [123]	– 1	3
N.W. Africa [124]	– 1	3
W. Equatorial Pacific [125]	– 1.5	3.5
Bering Sea [126]	– 1.5	1.5

* Altabet unpublished data, + Fig. 17

6 Summary and Synthesis

The major microbial transformation pathways within the marine N cycle have been well known for almost a century. Perception of a quasi-balanced biogeochemical system between sources and sinks was first made by Karl Brandt in 1902. Within the last three decades, serious and credible efforts have been made to quantify global ocean N fluxes and that with more detailed study estimates have almost been steadily revised upward. Particularly important were the respective discoveries of the importance of sedimentary denitrification and the dominance of oceanic N_2 fixation as a combined N source. In the last decade and a half, advances have been made in the application of geochemical tracers; objective analysis of NO_3^- anomalies and application of isotope natural abundance. It is not clear if there is modern balance between sources (primarily N_2 fixation) and losses (sedimentary and water denitrification) but total throughput is on the order of 200 to 400 Tg/yr with

a residence time for marine combined N < 3000 yrs. This is relatively short compared to other major biogeochemical cycles such as for P or Si. The N cycle is further distinguished by having the major source for combined N within the ocean and all major fluxes controlled by biological transformations. P and Si sources to the ocean, in contrast, are in primarily the form of riverine fluxes. Paleoceanographic reconstructions have clearly demonstrated large variations in water column denitrification coupled to climate change on time scales from hundreds to millions of years. In particular, increasing denitrification across the last deglaciation likely caused a significant change in the oceanic N inventory that in turn may have influenced atmospheric CO_2 and N_2O.

Important challenges remain in understanding the present past oceanic N cycle. It appears surprising that anammox as a potentially important pathway has only been recently recognized. Related problems include a reexamination of the stoichiometry of NO_3^- removal to N_2 production in open ocean denitrification. Greater certainty in sedimentary denitrification may be achieved by applying complementary geochemical approaches analogous to the applications made to N_2 fixation and water column denitrification. Perhaps just as important as establishing well-constrained flux estimates is achieving a realistic understanding of the controls and feedbacks within the oceanic N cycle that in turn determine total inventory when in quasi-steady state and the system's capacity for imbalance and transition to perhaps other states. Such mechanistic understanding must be based on further study in the modern of the factors to which denitrification and N_2 fixation are in reality most sensitive as well as paleoceanographic reconstructions to determine which states have been realized and their forcings.

Acknowledgements The author thanks Peng Feng and Rehka Singh for technical assistance in generating much of the data presented, Matt Higginson for thoughtful discussions and data analysis, Joe Montoya, Dave Murray, and Tim Herbert for on-going collaborations. The US NSF has provided the bulk of the support for the author's research group.

References

1. Liu KK (1979) Geochemistry of inorganic nitrogen compounds in two marine environments; the Santa Barbara Basin and the ocean off Peru. Doctoral Thesis, University of California, Los Angeles
2. Capone DG, Zehr JP, Paerl HW, Bergman B, Carpenter EJ (1997) Science 276:1221
3. Karl D, Michaels A, Bergman B, Capone D, Carpenter E, Letelier R, Lipschultz F, Paerl H, Stal L (2002) Biogeochemistry 57–58:47
4. Raven JA (1988) New Phytol 109:279
5. Kustka A, Sanudo-Wilhelmy S, Carpenter EJ, Capone DG, Raven JA (2003) J Phycol 39:12
6. Falkowski PG (1997) Nature 387:272

7. Sanudo-Wilhelmy SA, Kustka AB, Gobler CJ, Hutchins DA, Yang M, Lwiza K, Burns J, Capone DG, Raven JA, Carpenter EJ (2001) Nature 411:66
8. Mills MM, Ridame C, Davey M, La Roche J, Geider RJ (2004) Nature 429:292
9. Berman-Frank I, Cullen JT, Shaked Y, Sherrell RM, Falkowski PG (2001) Limnol Oceanogr 46:1249
10. Redfield A (1934) James Johnstone Memorial Volume, p 176
11. Gruber N, Sarmiento JL (1997) Glob Biogeochem Cycle 11:235
12. Deutsch C, Gruber N, Key RM, Sarmiento JL, Ganachaud A (2001) Global Biogeochem Cycle 15:483
13. Hansell DA, Bates NR, Olson DB (2004) Mar Chem 84:243
14. Bates NR, Hansell DA (2004) Mar Chem 84:225
15. Macko SA, Fogel ML, Hare PE, Hoering TC (1987) Chem Geol 65:79
16. Hoering T, Ford HT (1960) J Am Chem Soc 82:376
17. Delwiche CC, Zinke PJ, Johnson CM, Virginia RA (1979) Bot Gaz 140 (Suppl):s65
18. Mariotti A, Mariotti F, Amarger N, Pizelle G, Ngambi J-M, Champigny M-L, Moyse A (1980) Physiol Veg 18:163
19. Minagawa M, Wada E (1986) Mar Chem 19:245
20. Carpenter EJ, Harvey HR, Fry B, Capone DG (1997) Deep-Sea Res I 44:27
21. Sigman DM, Altabet MA, McCorkle DC, Francois R, Fischer G (2000) J Geophys Res-Oceans 105:19599
22. Sigman DM, Altabet MA, Michener R, McCorkle DC, Fry B, Holmes RM (1997) Mar Chem 57:227
23. Sigman DM, Casciotti KL, Andreani M, Barford C, Galanter M, Bohlke JK (2001) Anal Chem 73:4145
24. Casciotti KL, Sigman DM, Hastings MG, Bohlke JK, Hilkert A (2002) Anal Chem 74:4905
25. Richards FA (1965) In: Riley JP, Skirrow G (eds) Chemical Oceanography. Academic Press, London, p 611
26. Cohen Y, Gordon LI (1978) Deep-Sea Res 25:509
27. Christensen JP, Murray JW, Devol AH, Codispoti LA (1987) Glob Biogeochem Cycle 1:97
28. Deuser WG, Ross EH, Mlodzinska ZJ (1978) Deep Sea Res 25:431
29. Codispoti LA, Richards FA (1976) Limnol Oceanogr 21:379
30. Codispoti LA, Packard TT (1980) J Mar Res 38:453
31. Kuypers MMM, Sliekers AO, Lavik G, Schmid M, Jorgensen BB, Kuenen JG, Sinninghe Damsté JS, Strous M, Jetten MSM (2003) Nature 422:608
32. Dalsgaard T, Canfield DE, Petersen J, Thamdrup B, Acuna-Gonzalez J (2003) Nature 422:606
33. Codispoti L, Brandes J, Christensen J, Devol A, Naqvi S, Paerl H, Yoshinari T (2001) In: Gili J, Pretus J, Packard T (eds) A Marine Science Odyssey into the 21st Century (Scientia Marina), vol 65 (Suppl 2), p 85
34. Christensen JP, Smethie JW, Devol AH (1987) Deep-Sea Res 34:1027
35. Devol AH (1991) Nature 349:319
36. Brandes JA, Devol AH (2002) Glob Biogeochem Cycle 16:67
37. Miyake Y, Wada E (1971) Rec Oceanog Works Japan 11:1
38. Wellman RP, Cook FD, Krouse HR (1968) Science 161:269
39. Cline JD, Kaplan IR (1975) Mar Chem 3:271
40. Barford CC, Montoya JP, Altabet MA, Mitchell R (1999) Appl Environ Microbiol 65:989
41. Brandes JA, Devol AH, Yoshinari T, Jayakumar DA, Naqvi SWA (1998) Limnol Oceanogr 43:1680

42. Altabet MA, Murray DW, Prell WL (1999) Paleoceanography 14:732
43. Voss M, Dippner JW, Montoya JP (2001) Deep Sea Res II 48:1905
44. Brandes JA, Devol AH (1997) Geochim Cosmochim Acta 61:1793
45. Sigman DM, Robinson R, Knapp AN, Geen AV, McCorkle DC, Brandes JA, Thunell RC (2003) Geochem Geophys Geosyst 4:1
46. Wada E, Hattori A (1978) Geomicrobio J 1:85
47. Wada E (1980) In: Goldberg ED, Horibe Y (eds) Isotope Marine Chemistry. Uchida Rokakuho, Tokyo, p 375
48. Montoya JP, McCarthy JJ (1995) J Plank Res 17:439
49. Waser NA, Yin K, Yu Z, Tada K, Harrison PJ, Turpin DH, Calvert SE (1998) Mar Ecol Prog Ser 169:29
50. Needoba JA, Sigman DM, Harrison PJ (2004) J Phycol 40:517
51. Needoba JA, Harrison PJ (2004) J Phycol 40:505
52. Martin JH, Gordon RM, Fitzwater S, Broenkow WW (1989) Deep-Sea Res 36:649
53. Sigman DM, Boyle EA (2000) Nature 407:859
54. Chavez FP, Buck KR, Coale KH, Martin JH, DiTullio GR, Welschmeyer NA, Jacobson AC, Barber RT (1991) Limnol Oceanogr 36:1816
55. Sigman DM, Altabet MA, McCorkle DC, Francois R, Fischer G (1999) Glob Biogeochem Cycle 13:1149
56. Altabet MA, Francois R (2001) Deep-Sea Res II 48:4247
57. Checkley DM Jr, Entzeroth LC (1985) J Plank Res 7:553
58. Checkley DM Jr, Miller CA (1989) Deep-Sea Res 36:1449
59. DeNiro MJ, Epstein S (1981) Geochim Cosmochim Acta 45:341
60. Minagawa M, Wada E (1984) Geochim Cosmochim Acta 48:1135
61. Macko SA, Fogel Estep ML, Engel MH, Hare PE (1986) Geochim Cosmochim Acta 50:2143
62. McClelland JW, Montoya JP (2002) Ecology 83:2173
63. Saino T, Hattori A (1985) In: Sigleo AC, Hattori A (eds) Marine and Estuarine Geochemistry. Lewis Publishers, Chelsea, MI, p 697
64. Altabet MA (1988) Deep-Sea Res 35:535
65. Altabet MA (2001) Limnol Oceanogr 46:368
66. Altabet MA (1989) Limnol Oceanogr 24:1185
67. Altabet MA, Deuser WG, Honjo S, Stienen C (1991) Nature 354:136
68. Sweeney RE, Kaplan IR (1980) Mar Chem 9:81
69. Macko, Estep (1984) Org Geochem 6:787
70. Lehmann MF, Bernasconi SM, Barbieri A, McKenzie JA (2002) Geochim Cosmochim Acta 66:3573
71. Kendall C (1998) In: Kendall C, McDonnell JJ (eds) Isotope Tracers in Catchment Hydrology. Elsevier, Amsterdam, p 519
72. Lehmann MF, Sigman DM, Berelson WM (2004) Mar Chem 88:1
73. Yoshida N (1988) Nature 335:528
74. Cifuentes LA, Fogel ML, Pennock JR, Sharp JH (1989) Geochim Cosmochim Acta 53:2713
75. Horrigan SG, Montoya JP, Nevins JL, McCarthy JJ (1990) Est Coast Shelf Sci 30:393
76. Casciotti KL, Sigman DM, Ward BB (2003) 20:335
77. Goreau TJ, Kaplan WA, Wofsy SC, McElroy MB, Valois FW, Watson SW (1980) Appl Env Microbiol 40:526
78. Lipschultz F, Zafiriou OC, Wofsy SC, McElroy MB, Valois FW, Watson SW (1981) Nature 294:41
79. Nevison CD, Weiss RF, Erickson DJ (1995) J Geophys Res—Oceans 100:15809

80. Suntharalingam P, Sarmiento JL, Toggweiler JR (2000) Glob Biogeochem Cycle 14:353
81. Yoshinari T, Altabet MA, Naqvi SWA, Codispoti L, Jayakumar A, Kuhland M, Devol A (1997) Mar Chem 56:253
82. Popp BN, Westley MB, Toyoda S, Miwa T, Dore JE, Yoshida N, Rust TM, Sansone FJ, Russ ME, Ostrom NE, Ostrom PH (2002) Glob Biogeochem Cycle 16:12
83. Yoshida N, Toyoda S (2000) Nature 405:330
84. Goldman JC (1979) Microb Ecol 5:153
85. Goldman JC, McCarthy JJ (1978) Limnol Oceanogr 23:695
86. Quigg A, Finkel ZV, Irwin AJ, Rosenthal Y, Ho T, Reinfelder JR, Schofield O, Morel FMM, Falkowski PG (2003) Nature 425:291
87. Klausmeier CA, Litchman E, Daufresne T, Levin SA (2004) Nature 429:171
88. White AE, Letelier RM, Spitz YH (2003) J Phycol 39:59
89. Villareal T, Carpenter E (2003) Microb Ecol 45:1
90. Broecker WS (1982) Prog Oceanogr 11:151
91. Petit JR, Jouzel J, Raynaud D, Barkov NI, Barnola JM, Basile I, Beders M, Chappellaz J, Davis M, Delaygue G, Delmotte D, Kotlyakov VM, Legrand M, Lipenkov VY, Lorius C, Pepin L, Ritz C, Saltzman E, Stievenard M (1999) Nature 399:429
92. Knox F, McElroy M (1984) J Geophys Res 89:4629
93. Sarmiento J, Toggweiler R (1984) Nature 308:621
94. Sieganthaler, Wenk (1984) Nature 308:624
95. Martin JH (1990) Paleoceanogr 5:1
96. Francois R, Altabet MA, Yu E-F, Sigman D, Bacon MP, Frank M, Bohrmann G, Barielle G, Labeyrie L (1997) Nature 389:929
97. Sigman DM, Altabet MA, Francois R, McCorkle DC, Gaillard JF (1999) Paleoceanogr 14:118
98. McElroy M (1983) Nature 302:328
99. Anschutz P, Sundby B, Lefrancois L, Luther GW, Mucci A (2000) Geochim Cosmochim Acta 64:751
100. Altabet MA, Curry WB (1989) Glob Biogeochem Cycle 3:107
101. Eppley RW, Peterson BJ (1979) Nature 282:677
102. Altabet MA, McCarthy JJ (1985) Deep-Sea Res 32:755
103. Crosta X, Shemesh A (2002) Palaeoceanogr 17:10
104. Sachs JP, Repeta DJ, Goericke R (1999) Geochim Cosmochim Acta 63:1431
105. Sachs JP, Repeta DJ (1999) Science 286:2485
106. Keil RG, Fogel ML (2001) Limnol Oceanogr 46:14
107. Altabet MA, Francois R, Murray DW, Prell WL (1995) Nature 373:506
108. Altabet M, Higginson M, Murray DW (2002) Nature 415:159
109. Ganeshram RS, Pedersen TF, Calvert SE, Murray JW (1995) Nature 376:755
110. Ganeshram RS, Pedersen TF, Calvert SE, McNeill GW, Fontugne MR (2000) Paleoceanogr 15:36
111. Kienast SS, Calvert SE, Pedersen TF (2002) Paleoceanogr 17:1055
112. Dansgaard W, Clausen HB, Gundestrup N, Hammer CU, Johnsen SF, Kristinsdottir PM, Reeh N (1982) Science 218:1273
113. Morford JL, Emerson S (1999) Geochim Cosmochim Acta 63:1735
114. Hendy IL, Kennett JP (2003) Quat Sci Rev 22:673
115. Raymo ME, Nisancioglu K (2003) Paleoceanogr. 18:1011
116. Ohkouchi N, Eglinton TI, Keigwin LD, Hayes JM (2002) Science 298:1224
117. Kanfoush SL, Hodell DA, Charles CD, Janecek TR, Rack FR (2003) Palaeogeogr Palaeoclim Palaeoecol 182:329

118. Codispoti LA, Elkins JW, Yoshinari T, Friederich GE, Sakamoto CM, Packard TT (1992) In: Desai BN (ed) Oceanography of the Indian Ocean. Oxford and IBH Publishing Co., New Dehli, p 271
119. Suthhof A, Ittekkot V, Gaye-Haake B (2001) Glob Biogeochem Cycle 15:637
120. Kienast M (2000) Paleoceanogr 15:244
121. Higginson MJ, Maxwell JR, Altabet MA (2003) Mar Geol 201:223
122. Holmes ME, Schneider RR, Muller PJ, Segl M, Wefer G (1997) Paleoceanogr 12:604
123. Schubert CJ, Stein R, Calvert SE (2001) Paleoceanogr 16:199
124. Martinez P, Bertrand P, Calvert S, Pedersen T, Shimmield G, Lallier-Verges E, Fontugne M (2000) J Mar Res 58:809
125. Nakatsuka T, Harada N, Matsumoto E, Handa N, Oba T, Ikehara M, Matsuoka H, Kimoto K (1995) Geophys Res Lett 22:2525
126. Nakatsuka T, Watanabe K, Handa N, Matsumoto E, Wada E (1995) Paleoceanogr 10:1047
127. Nelson JR, Beers JR, Eppley RW, Jackson GA, McCarthy JJ, Soutar A (1987) Cont Shelf Res 7:307
128. Haug GH, Pedersen TF, Sigman DM, Calvert SE, Nielsen B, Peterson LC (1998) Paleoceanogr 13:427
129. Altabet MA, Pilskaln C, Thunell R, Pride C, Sigman D, Chavez F, Francois R (1999) Deep-Sea Res 46:655
130. Voss M, Altabet MA, Bodungen BV (1996) Deep-Sea Res II 43:33
131. Velinsky DJ, Fogel MF (1999) Mar Chem 67:3
132. Holmes ME, Muller PJ, Schneider RR, Segl M, Patzold J, Wefer G (1996) Mar Geol 134:1
133. Thunell RC, Kepple AB (2004) Glob Biogeochem Cycle 18:1001
134. Nakatsuka T, Handa N (1997) J Oceanogr 53:105
135. Pantoja S, Repeta DJ, Sachs JP, Sigman DM (2002) Deep-Sea Res I 49:1609
136. Antia AN, Maassen J, Herman P, Voss M, Scholten J, Groom S, Miller P (2001) Deep-Sea Res II 48:14
137. Kerherve P, Minagawa M, Heussner S, Monaco A (2001) Oceanol Acta 24 S:S77
138. Karl D, Letelier R, Tupas L, Dore J, Christian J, Hebel D (1997) Nature 388:533
139. Fry B, Jannasch HW, Molyneaux SJ, Wirsen CO, Muramoto JA, King S (1991) Deep-Sea Res A 38:S1003
140. Liu K-K, Kaplan IR (1989) Limnol Oceanogr 34:820
141. Smith SL, Henrichs SM, Rho T (2002) Deep-Sea Res II 49:6031
142. Wong GTF, Chung S-W, Shiah F-K, Chen C-C, Wen L-S, Liu K-K (2002) Geophys Res Lett, 29:1029
143. Robinson RS, Brunelle BG, Sigman DM (2004) Paleoceanogr 19:3001
144. Indermuhle A, Monnin E, Stauffer B, Stocker TF, Wahlen M (2000) Geophys Res Lett 27:735